



Structural framework and timing of the Pahtohavare Cu ± Au deposits, Kiruna mining district, Sweden

Leslie Logan, Ervin Veress, Joel B. H. Andersson, Olof Martinsson, and Tobias E. Bauer

Division of Geosciences and Environmental Engineering, Luleå University of Technology, Luleå 971 87, Sweden

Correspondence: Leslie Logan (leslie.logan@ltu.se)

Received: 20 December 2022 – Discussion started: 9 January 2023

Revised: 22 May 2023 – Accepted: 27 May 2023 – Published: 18 July 2023

Abstract. As part of the larger mineral systems approach to Cu-bearing mineralization in northern Norrbotten, this study utilizes structural geology to set the classic Pahtohavare Cu ± Au deposits into an up-to-date tectonic framework. The Pahtohavare Cu ± Au deposits, situated only 5 km southwest of the Kiirunavaara world-class iron oxide–apatite (IOA) deposit, have a dubious timing, and their link to IOA formation is not constrained. The study area contains both epigenetic Cu ± Au (Pahtohavare) and iron oxide–copper–gold (IOCG; Rakkurijärvi) mineral occurrences which are hosted in bedrock that has been folded and bound by two shear zones trending northeast to southwest and northwest to southeast to the east and southwest, respectively. Structural mapping and petrographic investigation of the area reveal a noncylindrical, SE-plunging anticline. The cleavage measurements mirror the fold geometry, which characterizes the fold as F_2 associated with the late phase of the Svecofennian orogeny. Porphyroclasts with pressure shadows, mylonitic fabrics, and foliation trails in porphyroblasts indicate S_0/S_1 is a tectonic fabric. The epigenetic Pahtohavare Cu ± Au mineralization sits in brittle–ductile structures that cross-cut an earlier foliation and the F_2 fold, indicating that the timing of the deposits occurred syn- to post- F_2 folding, at least ca. 80 Myr after the Kiirunavaara IOA formation. A 3D model and cross-sections of the Pahtohavare–Rakkurijärvi area and a new structural framework of the district are presented and used to suggest that the shear zones bounding the area are likely reactivated early structures that have played a critical role in ore formation in the Kiruna mining district.

1 Introduction

Globally, there has been a growing interest in research on clarifying the genetic relationship between iron oxide–apatite (IOA) and iron oxide–copper–gold (IOCG) deposits. Several studies from the Chilean iron belt, the Great Bear Magmatic Zone, and the St. Francois Mountains terrane in southeastern Missouri argue that IOA and IOCG deposits form from a single evolving magmatic–hydrothermal or hydrothermal fluid during one ore-forming event (see Corriveau et al., 2016; Day et al., 2016; Barra et al., 2017; Simon et al., 2018), building on the concept that IOA deposits may represent the deeper roots of a spectrum between an IOA–IOCG mineral system (Sillitoe, 2003). However, other researchers argue that these two deposit types have distinct geneses despite sharing similar geologic environments and characteristics (e.g., Williams et al., 2005; Groves et al., 2010; Tornos, 2011; Barton, 2014; Martinsson et al., 2016; Skirrow, 2021). For example, some researchers favor a purely orthomagmatic model for IOA deposits (e.g., Nyström and Henriquez, 1994; Naslund et al., 2002; Velasco et al., 2016; Tornos et al., 2017; Troll et al., 2019), a model that is incongruous for some IOCG deposits in which a magmatic–hydrothermal fluid and/or metal source is indirect or ambiguous (see Barton, 2014).

The Kiruna mining district is situated in the northern Norrbotten ore province (Martinsson et al., 2016), which has abundant Fe and Cu–Au mineralization, extensive Na–Ca metasomatism (Frietsch et al., 1997), and regional crustal-scale fault structures (Bergman et al., 2001). Multiple styles of mineralization are hosted in Rhyacian to Orosirian rocks with major ore-forming periods related to the Orosirian Svecofennian orogeny (ca. 1.9 to 1.8 Ga; Bergman et al., 2001; Martinsson et al., 2016). The orogeny was polyphase and re-

sulted in complex reactivation of structures and overprinting metamorphic events, alteration assemblages, and mineralization regionally (e.g., Wright, 1988; Bergman et al., 2001; Wanhainen et al., 2012; Martinsson et al., 2016; Bergman, 2018; Andersson et al., 2021; Bauer et al., 2022). Radiometric studies point to abundant IOA and Cu–Au mineralization processes during the early-orogenic phase of the Svecokarelian orogeny (ca. 1880–1860 Ma; Cliff et al., 1990; Romer et al., 1994; Wanhainen et al., 2005; Smith et al., 2007, 2009; Westhues et al., 2016; Martinsson et al., 2016); however increasing structural evidence links a generation of Cu ± Au mineralization to brittle structures constrained to a late phase of the tectonic evolution (Bauer et al., 2018, 2022; Andersson et al., 2020, 2021), supported by radiometric studies (Storey et al., 2007; Martinsson et al., 2016; Sarlus et al., 2018; Andersson et al., 2022). For example, Bauer et al. (2018, 2022) use structural constraints on alteration and mineralization to show that Cu–Au mineralization in the Nautanen deformation zone and the Malmberget IOA deposit is hosted in late-orogenic structures, and they suggest that either a late mineralization with new metal input occurred, or tectonically late structures acted as traps for remobilized metals. These findings raise an important question about the relative timing of Cu ± Au introduction and/or remobilization in the Norrbotten ore province and how IOA mineralizing systems are related to Cu–Au occurrences in the context of the tectonic evolution.

In the southern Kiruna mining district, structurally and lithologically controlled, stratabound to discordant Cu ± Au deposits are known in the Pahtohavare area (Martinsson et al., 1997a) and occur ca. 2 km northwest of the Rakkurijärvi iron oxide–copper–gold (IOCG) deposit. These Fe ± Cu ± Au deposits are situated 5 km southwest of the world-class Kiirunavaara IOA deposit, which has received over 100 years of scientific spotlight (e.g., Geijer, 1910; Lundbohm, 1910; Parák, 1975; Cliff et al., 1990; Cliff and Rickard, 1992; Nyström and Henriquez, 1994; Westhues et al., 2016), while the Fe ± Cu ± Au occurrences in the district have relatively few dedicated studies (e.g., Viscaria, Rakkurijärvi, Pahtohavare; Lindblom et al., 1996; Martinsson et al., 1997a, b; Smith et al., 2007). The Kiirunavaara IOA deposit has an accepted age of ca. 1880 Ga (Welin, 1987; Cliff et al., 1990; Romer et al., 1994; Smith et al., 2009; Westhues et al., 2016; Martinsson et al., 2016) and has been structurally constrained to the early extensional phase of the Svecokarelian orogeny (Andersson et al., 2021); however, the timing and structural setting of the Pahtohavare deposits are unknown. The main purpose of this study is to determine the relative timing of the formation of the Pahtohavare Cu ± Au deposits by conducting a structural investigation of the area and contextualizing the results within the district and regional tectonic frameworks as a part of a broader mineral systems approach (Wyborn et al., 1994). A well-characterized regional structural framework offers a tool for unraveling the relative timing of events where multiple generations of simi-

lar alteration and mineralization styles may overprint each other, where isotopic systems used for radiometric dating are subject to disturbance, or where datable phases in relevant textural positions are lacking. The results from this work add important data to the debate about the genesis of IOA and IOCG deposits and whether they necessarily form coevally and under the same tectonic conditions. Furthermore, increased understanding of the timing and structural setting of Cu ± Au deposits in Norrbotten is important for exploration. This study adds significant new data from the southern Kiruna mining district, where limited structural information has been published (Martinsson et al., 1993).

2 Geological setting

The descriptions of the rocks used in this paper follow the nomenclature presented by Martinsson (2004). The rocks in northern Sweden (Fig. 1) are metamorphosed from greenschist to amphibolite facies conditions; however, the “meta” prefix is excluded for clarity and emphasis on the original protolith.

2.1 Regional geologic setting

2.1.1 Neoproterozoic buildup and early-Paleoproterozoic rifting

The Norrbotten craton basement rocks comprise Neoproterozoic (ca. 2.9–2.6 Ga) gneissic granitoids of tonalitic to granodioritic composition, amphibolites, and paragneisses (Martinsson et al., 1999; Bergman et al., 2001) which formed during the continental buildup of the Lopian orogeny (Bergman et al., 2001). The southwestern boundary of the Archean crust has been traced using ϵNd values in Paleoproterozoic plutonic–volcanic rocks (Öhlander et al., 1993) that broadly define the margin as running from the Bothnian Bay south of Luleå, towards the northwest through Jokkmokk, hence, the Luleå–Jokkmokk line (Mellqvist, 1999; Fig. 1).

The early Paleoproterozoic marked major rifting events of the basement which created NW–SE-oriented, first-order structures (Skyttä et al., 2019). Tholeiitic volcanic and volcanoclastic rocks and rift-related sedimentary successions were generated from ca. 2.5–2.0 Ga and formed a greenstone belt that extends today from northern Norway to Russian Karelia (Pharaoh and Pearce, 1984; Martinsson, 1997; Bingen et al., 2015). The greenstone successions are important hosts for syn- to post-depositional Fe, Cu, and Cu ± Au mineralization regionally (Martinsson et al., 2016).

2.1.2 Svecokarelian early-orogenic extension and crustal shortening

Around 1.90 Ga, NE-directed subduction (BABEL Working Group, 1990; Öhlander et al., 1993) and back-arc extension (Pharaoh and Pearce, 1984; Andersson et al., 2021; Bauer et

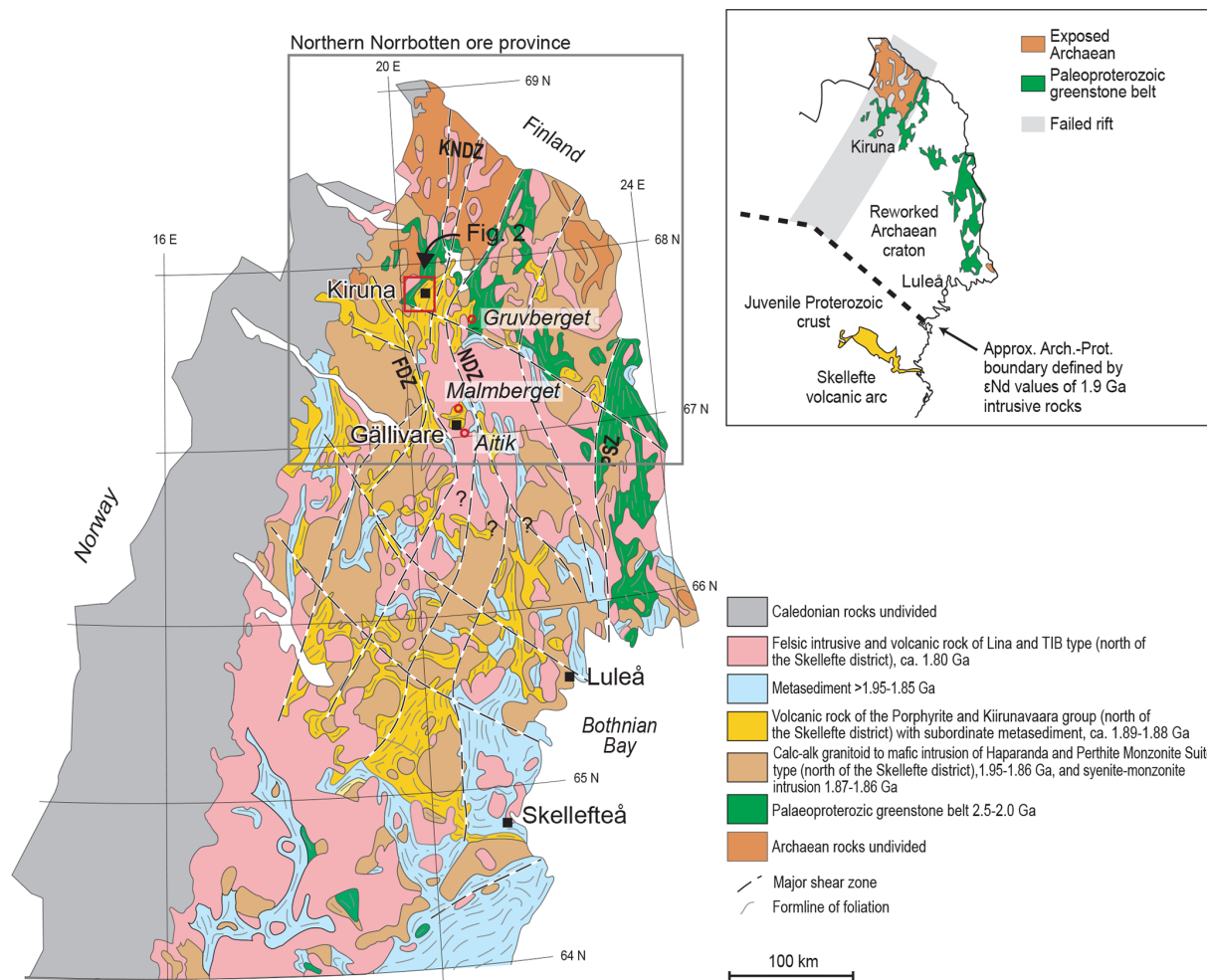


Figure 1. Geologic map of northern Sweden with both the Skellefte district and the northern Norrbotten ore province included. Inset shows approximate paleoboundary of the Archean craton defined by ϵ Nd values (Öhlander et al., 1993). FDZ: Fjällåsen deformation zone; KNDZ: Kiruna-Naimakka deformation zone; NDZ: Nautanen deformation zone; PSZ: Pajala shear zone. Modified after Bauer et al. (2022), Weihed and Williams (2005), and Bauer and Andersson (2021).

al., 2022) began along the southern margin of the Archean craton, marking the start of the polyphase Sveco Karelian accretionary orogenic cycle (Bergman et al., 2001). Several deformation, metamorphic, and magmatic events are recorded in the Norrbotten lithotectonic unit, accompanied by varying degrees of hydrothermal alteration and mineralization (see Bergman et al., 2001; Martinsson et al., 2016; Grigull et al., 2018; Luth et al., 2018b; Bauer et al., 2018, 2022; Bergman and Weihed, 2020; Andersson et al., 2020, 2021). The associated magmatic suites are the calc-alkaline to alkali-calcic Haparanda suite–Porphyrite group and Perthite monzonite suite (PMS)–Kiirunavaara group, which vary from mafic to felsic rock types in the northern Norrbotten area (Perdahl and Frietsch, 1993; Bergman et al., 2001; Martinsson, 2004; Sarlus et al., 2020; Logan et al., 2022). Abundant Na–Ca metasomatism related to the elevated thermal flux from the intrusive activity and fluids channeling through faults resulted in

the formation of albite, marialitic scapolite, magnetite, amphibole, and carbonate (Frietsch et al., 1997; Bergman et al., 2001; Martinsson et al., 2016; Andersson et al., 2020). Early mineral deposits formed during this time include IOA (e.g., Kiirunavaara), porphyry Cu (Au–Ag–Mo) (e.g., Aitik), and IOCG (e.g., Rakkurijärvi; Smith et al., 2007, 2009; Wanhainen et al., 2005; Westhues et al., 2016).

The accretion of the Skellefte volcanic arc to the Archean craton to the north (Hietanen, 1975; Skiöld, 1988; Öhlander et al., 1993; Weihed et al., 2002; Bergman and Weihed, 2020; Skyttä et al., 2020) resulted in crustal shortening from ca. 1.88–1.86 Ga (termed D_1 in Norrbotten but D_2 in the Skellefte district and Överkalix lithotectonic unit; Skyttä et al., 2012; Bergman and Weihed, 2020). The movement along shear zones is less known from this event, but kinematic data from approximately 40 km southwest of Kiruna (Fig. 1) suggest that reverse–oblique sinistral movement occurred (An-

dersson et al., 2020). A penetrative, but heterogeneously developed, dominantly NW–SE-striking tectonic fabric formed from an inferred NE–SW-shortening direction under mostly plastic conditions (Grigull et al., 2018; Bauer et al., 2018, 2022; Andersson et al., 2020). The tectonic fabric is interpreted to have formed under peak metamorphism (lower amphibolite) recorded by syn-tectonic growth of hornblende (Andersson et al., 2020), though regionally the metamorphic grade can be higher (Bergman et al., 2001). Amphibolite facies metamorphism characterizes M₁ in Norrbotten, except in the Kiruna mining district, which shows a lower overall metamorphic grade characterized by upper greenschist facies metamorphism, though local transitions to lower amphibolite facies occur (Bergman et al., 2001; Andersson et al., 2021, 2022). In the Skellefte district a 1.87 Ga basin inversion is observed (Bauer et al., 2011; Skyttä et al., 2012); however, it is not recorded or is masked in the Kiruna mining district (Andersson et al., 2021).

2.1.3 Svecokarelian late-orogenic crustal shortening

A second phase of subduction was initiated around 1.81–1.78 Ga, coeval with abundant crustal melting and emplacement of silica-rich granites of the Lina suite and quartz-poor monzonitic A-/I-type granitoids, syenites, and gabbros of the Transscandinavian Igneous Belt (Bergman et al., 2001; Högdahl et al., 2004; Bergman et al., 2006; Martinsson et al., 2018; Sarlus et al., 2018). Metamorphism has been suggested to be of low-pressure, high-temperature conditions during this orogenic phase due to the occurrence of brittle structures and folding with only locally developed, spaced axial-plane-parallel fabric, together with higher-temperature minerals (e.g., cordierite, garnet; Bergman et al., 2001; Bauer et al., 2018; Skelton et al., 2018). Additionally, K to K–Fe metasomatism/alteration can be found in late-orogenic (D₂) shear zones and brittle fractures (Andersson et al., 2020; Bauer et al., 2022) and occurs in spatial proximity to late-orogenic intrusions and pegmatites or as a result of late magmatic–hydrothermal activity (Andersson et al., 2020; Bauer et al., 2018, 2022). The second deformation event was inhomogeneous and confined to major deformation zones from E–W crustal shortening (e.g., Bergman et al., 2001; Weihed et al., 2002; Lahtinen et al., 2005; Bauer et al., 2018; Luth et al., 2018b; Andersson et al., 2021). In general, kinematic data show steep east-side-up movement along the shear zones in the east, while in the west dominantly west-side-up kinematics are observed (Bergman et al., 2001; Lynch et al., 2015; Luth et al., 2018b; Andersson et al., 2020). The event is associated with brittle–plastic conditions producing spaced S₂ cleavages and strong strain partitioning (Grigull et al., 2018; Luth et al., 2018b; Bauer et al., 2018, 2022; Andersson et al., 2020).

The second phase of deformation was followed by a clockwise rotation of the stress field to a NNW–SSE- to N–S-oriented crustal shortening direction (D₃), which caused a

gentle refolding of preexisting fabrics and crenulation of white mica and chlorite domains recorded in the Kiruna area (Andersson et al., 2021). A similar orientation of crustal shortening related to this deformation event is recorded in the Pajala area to the east; however it differs from that seen in Kiruna by the resultant formation of WNW–ESE and NNW–SSE conjugate faults (Luth et al., 2018a).

2.1.4 Late-Svecokarelian deformation

A late deformation event is observed in both Kiruna and the Gällivare area (approximately 70 km to the south; Fig. 1) that is characterized by brittle fracturing (Romer, 1996; Bauer et al., 2018; Andersson et al., 2021). At the Luossavaara and Rektor IOA deposits in the Kiruna mining district (Fig. 2), this event is structurally constrained by a calcite–quartz hydraulic breccia that cross-cuts S₂ fabrics (Andersson et al., 2021). Additionally, radiometric U–Pb age constraints on monazite from the Rektor and Kiirunavaara ores identify a late hydrothermal event at ca. 1.74–1.72 Ga and ca. 1.62 Ga (Blomgren, 2015: laser ablation inductively coupled plasma mass spectroscopy, LA-ICP-MS; Westhues et al., 2017: secondary-ion mass spectrometry, SIMS). In Kiruna, U–Pb (single-collector inductively coupled plasma ionization mass spectrometer, SC-ICP-MS) ages from monazite in hydrothermal calcite found in the Kiruna-Naimakka deformation zone indicate an event at ca. 1.78–1.76 Ga (Lauri et al., 2022). At Malmberget, in the Gällivare area (Fig. 1), low-temperature hydrothermal monazite and stilbite associated with late calcite-bearing brittle fractures yield U–Pb crystallization ages between ca. 1.74–1.73 Ga, with associated apatite and titanite showing a later recrystallization and/or hydrothermal event around ca. 1.60–1.62 Ga (isotope dilution thermal ionization mass spectrometry, ID-TIMS; Romer, 1996).

2.2 Local geology

2.2.1 Stratigraphy and intrusive rocks

The Kiruna mining district, outlined in Fig. 2, has a well-preserved lithostratigraphic sequence from Archean to Orosirian age and has previously been comprehensively described by Lundbohm (1910), Frietsch (1979), Martinsson (2004), and Andersson et al. (2021). The lowermost part of the sequence includes an Archean granite (ca. 2.7 Ga; Logan et al., 2022) which occurs in a small occurrence in the southern part of the district (Fig. 2) and is unconformably overlain by Rhyacian greenstone rocks and later-Orosirian rocks (Martinsson, 1997). The lowermost succession of greenstones belongs to the ca. 2.5–2.3 Ga Kovo group, comprising basal clastic sedimentary rocks, basaltic lavas, volcanogenic graywackes, and a series of tholeiitic to calc-alkaline volcanic rocks (Martinsson, 1997). Above the Kovo group lies the Kiruna greenstone group, which consists

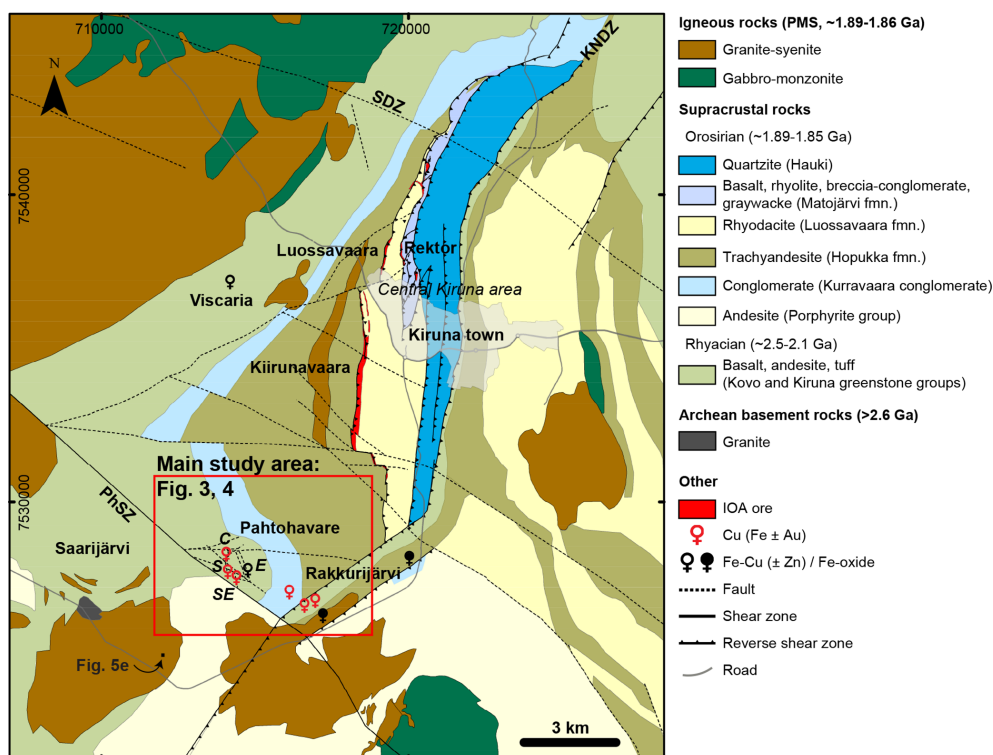


Figure 2. Geologic map of the Kiruna mining district showing stratigraphy, structures, and igneous intrusions. The town of Kiruna is marked in transparent gray. Cu (Fe ± Au), Fe–Cu (± Zn), and Fe-oxide occurrences are shown as well as local area names. Pahtohavare deposits: C – Central, E – Eastern, S – Southern, SE – Southeastern. KNDZ: Kiruna-Naimakka deformation zone; PhSZ: Pahtohavare shear zone; SDZ: Svappavaara deformation zone. Modified after Martinsson et al. (1993) and Andersson et al. (2021). Coordinate system in SWEREF99.

of basaltic lavas, conglomerates, and dolostones at the base and is overlain by komatiitic to tholeiitic volcanics, tholeiitic to calc-alkaline volcano-sedimentary formations, graphite schists, and pillow basalts (Martinsson, 1997). Mafic sills related to the pillow basalt formation occur within the volcanoclastic unit (Martinsson, 1997).

The mid-Orosirian rocks related to the early-Svecokarelian orogenic cycle overlie the greenstones with the unconformable Kurravaara conglomerate at the base (Fig. 2). This formation is polymictic and poorly sorted, with rounded to subrounded clasts approximately 0.5 to >10 cm (locally up to 50 cm) in size (Frietsch, 1979). A volcanic intercalation in the Kurravaara conglomerate has been radiometrically dated (U–Pb zircon SIMS), which constrains the minimum age of the conglomerate to ca. 1.89 Ga (Andersson et al., 2021). In some areas, andesitic volcanic rocks of the Porphyrite group are the lowermost unit of the Orosirian stratigraphy and represent the extrusive products of early arc magmatism (Martinsson and Perdahl, 1995; Martinsson, 2004).

Overlying these basal units are the volcanic rocks of the Kiirunavaara group, including the trachyandesitic Hopukka formation and dacitic–rhyolitic Luossavaara formation, which make up the footwall and hanging wall, re-

spectively, to the giant Kiirunavaara IOA deposit (Fig. 2; Martinsson 2004). The Matojärvi formation overlies the Luossavaara formation and consists of a series of rhyolitic tuffs, basaltic lavas, alluvial breccia conglomerates, graywackes, and phyllites (Fig. 2; Lundbohm, 1910; Frietsch, 1979; Martinsson, 2004; Andersson et al., 2021). This formation is overlain by quartz–feldspar arenites with intercalations of alluvial breccia conglomerates forming the Hauki quartzite (Fig. 2; Lundbohm, 1910; Martinsson, 2004).

Distributed through the Kiruna mining district are mafic to felsic plutonic intrusions (Offerberg, 1967), regarded as comagmatic with the Kiirunavaara group volcanic rocks (Hopukka and Luossavaara formations) and suggested to belong to the PMS (Witschard, 1984; Martinsson, 2004). Radiometric dating (U–Pb zircon by ID-TIMS and SIMS) of these intrusions verifies an early-orogenic timing (ca. 1.90–1.86 Ga) of magmatic activity (Cliff et al., 1990; Westhues et al., 2016; Logan et al., 2022). Only one U–Pb radiometric determination (ID-TIMS zircon and titanite, 1792 ± 4 Ma) has indicated a late-orogenic age for a syenitic intrusion in the district (Romer et al., 1994); however recent geochronological work from the area could not confirm the timing (1880 ± 7 Ma; Logan et al., 2022), making the presence of a late-orogenic intrusive body enigmatic.

2.2.2 Local structures

Structurally, the rock sequence and structural features in the Kiruna mining district strike north to northeast and dip steeply to the east (Fig. 2). The district lies adjacent to the Kiruna-Naimakka deformation zone (KNDZ), which runs approximately north to south throughout Norrbotten (Figs. 1, 2). Several undulating, approximately N–S- to NE–SW-trending, E-dipping reverse shear zones related to the KNDZ occur parallel to lithostratigraphic boundaries (Andersson et al., 2021) such as at the upper boundary of the Hauki quartzite (Fig. 2). East of the Hauki quartzite a thin unit of greenstones is repeated (Fig. 2), a feature also observed in the Rakkurijärvi area. The shear zones show east-side-up kinematics (Andersson et al., 2021), and the earliest direct age determination of deformation in the district comes from fracture-plane-hosted hydrothermal titanite in an approximately NNE–SSW-trending cataclastic fault damage zone at the Luossavaara IOA deposit (Fig. 2), showing the minimum age of fault initiation to be 1889 ± 26 Ma (Andersson et al., 2022). This is interpreted to represent syn-volcanic faulting during the basin evolution of the early Svecofokarelian. The N–S shear zones are interpreted to have been active during the first crustal shortening phase of the Svecofokarelian orogeny based on radiometric age results of the Rakkurijärvi IOCG deposit at ca. 1.86 Ga (Re–Os molybdenite and U–Pb LA-ICP-MS allanite, U–Pb TIMS rutile; Smith et al., 2007, 2009; Martinsson et al., 2016), the mineralization for which has been described to be controlled by the adjacent NE–SW-trending fault zone (Smith et al., 2007). Despite evidence of the faults being active at this time, the Orosirian portion of the stratigraphic sequence in the central Kiruna area (approximately the transect from the Luossavaara IOA deposit through the Hauki quartzite; see Andersson et al., 2021; Fig. 2) is reported to lack early-orogenic deformation fabrics (S_1 ; Andersson et al., 2021). The structures in the district predominantly record late-orogenic E–W crustal shortening (resulting in east-side-up kinematics), basin inversion, and S_2 foliation (Andersson et al., 2021). Strain partitioning commonly characterizes this event and has resulted in non-coaxial strain focused into lithological contacts and rheologically weak rocks such as those in the Matojärvi formation, which represents a high-strain zone with highly tectonized and mylonitic rocks (Andersson et al., 2021). In contrast, competent rocks record limited finite strain and have deformed through brittle faulting and fracturing (Andersson et al., 2021). U–Pb (LA-ICP-MS) age dating on syn-tectonic titanite from a brittle–ductile reverse shear zone with east-side-up kinematics approximately 6 km east of the Kiirunavaara IOA deposit constrain the age of late-Svecofokarelian crustal shortening to between 1812 ± 3 Ma and 1802 ± 8 (Andersson et al., 2021, 2022).

Following the E–W crustal shortening event, a N–S gentle refolding phase is recorded in the district, mainly observed in crenulated chlorite–white mica domains and in folded fabrics

with steep to shallow E-plunging fold axes (Andersson et al., 2021). This was followed by a late brittle event that cross-cuts all earlier fabrics and in the Kiruna mining district is found only locally (Andersson et al., 2021). These include hydraulic fracturing with calcite–quartz infill (Andersson et al., 2021, Lauri et al., 2022) and remobilization of apatite into veins (Andersson et al., 2021).

2.2.3 Local ore deposits

The Kiruna mining district is host to Kiruna-type IOA deposits and a variety of Cu mineralization, including stratiform–stratabound Fe–Cu (\pm Zn) deposits (i.e., Viscaria, Eastern Pahtohavare; Martinsson et al., 1997b), epigenetic stratabound to discordant Cu \pm Au deposits (Southern, Southeastern, and Central Pahtohavare; Martinsson et al., 1997a), and IOCG-style deposits (Rakkurijärvi; Smith et al., 2007). While different genetic models exist, thorough structural assessments of the copper deposits are lacking.

The area is best known for the giant Kiirunavaara IOA deposit that has been actively mined for iron ore for over a century (Fig. 2). The deposit is a tabular body of low-Ti magnetite–apatite ore with brecciated hanging and footwall contact zones (Geijer, 1919; Bergman et al., 2001; Martinsson and Hansson, 2004) and is situated along the lithological contact between the Hopukka and Luossavaara formations. U–Pb radiometric data constrain the timing of the ore formation through the dating of host rocks, ore minerals, and alteration minerals to ca. 1880 Ma (Welin, 1987; Cliff et al., 1990; Romer et al., 1994; Smith et al., 2009; Westhues et al., 2016; Martinsson et al., 2016). However, only recently has the structural context of the ore system been incorporated into a genetic model, with the emplacement of IOA deposits suggested to be coeval with syn-volcanic faulting (1889 ± 26 Ma, titanite U–Pb LA-ICP-MS) during early-orogenic basin development and back-arc extension (Andersson et al., 2022).

The Rakkurijärvi deposits (ca. 1.86 Ga; Smith et al., 2007, 2009; Martinsson et al., 2016) occur spatially associated with a NE–SW-trending shear zone approximately 5 km south-southwest of the Kiirunavaara IOA (Fig. 2) and have been described to be IOCG-style deposits (Smith et al., 2010). The ore bodies are hosted in both the Kurravaara conglomerate, which occurs to the northwestern side of the shear zone, and in the Kiirunavaara group volcanics (e.g., Hopukka formation) on the SE side (Smith et al., 2007). Chalcopyrite is the main ore-bearing sulfide and was precipitated with calcite in the matrix of brecciated massive magnetite and of lithic breccias (Smith et al., 2007). Selectively pervasive magnetite replacement of conglomerate clasts with Cu mineralization within the Kurravaara conglomerate suggests that some mineralization is a product of hydrothermal alteration (Smith et al., 2007).

The deposits at Pahtohavare (four sub-localities: Eastern, Southern, Southeastern, and Central; Fig. 2) are situated in

the Kiruna greenstone group approximately 5 km southwest of the Kiirunavaara IOA. The host rocks are folded into a SE-plunging anticline, with the oldest formations located in the core. They are truncated on the southwest by a NW–SE-trending shear zone (Fig. 2). The kinematics of the shear zone are currently unknown. The earliest mineralization (Eastern Pahtohavare) is suggested to have formed during the deposition of the greenstones (ca. 2.1 Ga) in an exhalative environment based on the stratiform character, alteration in the foot-wall, and Cu/Zn zonation (Martinsson et al., 1997b). The Southern, Southeastern, and Central Pahtohavare deposits are epigenetic and formed after the deposition of the greenstone rocks. The Southern and Southeastern deposits were mined over a period of 7 years during the 1990s and produced 1.7 Mt of ore with 1.9% Cu and 0.9 ppm Au (Martinsson et al., 1997a) and are the main focus of this study. The Central deposit is unmined and dominated by secondary oxidized mineral assemblages.

The epigenetic ore bodies are both structurally and lithologically controlled (Martinsson et al., 1997a). The Southern deposit is situated in the southern limb of the anticline (Fig. 2), and the ore body is bound by tectonic contacts with the geometry being fault-controlled (Martinsson et al., 1997a). However, the mineralization is lithologically constrained to pervasively albite-altered graphite schist and tuffite units (Martinsson et al., 1997a). The ore minerals include chalcopyrite and pyrite disseminated in the albite-altered rocks, as well as in cataclastic and hydrothermal veins and breccia fillings composed of ferrodolomite–quartz–pyrite–chalcopyrite (Martinsson et al., 1997a). The Southeastern deposit is located in the upper part of the volcanoclastic units of the Kiruna greenstone group (upper Viscaria formation) near the crest of the anticline (Fig. 2; Martinsson et al., 1997a). Lithologically, it is stratabound within pervasively albite-altered mafic–intermediate tuffites and thin graphite schist intercalations but has a distinct NNW-directed subvertical shear zone, with discordant mineralization that cuts the host rocks at a high angle (Martinsson et al., 1997a). The mineralization in the stratabound albite-altered zone occurs disseminated as chalcopyrite and pyrite and as veinlets and breccia infill. In the discordant ore zone the mineralization occurs in a coarse-grained ferrodolomite–quartz–scapolite–albite–chalcopyrite–pyrite vein with mylonitic to cataclastic textures (Martinsson et al., 1997a). The ages of the Pahtohavare deposits have not been determined radiometrically; however, they have been suggested to be of a similar age to the Rakkurijärvi deposit based on the geochronological results (1859 ± 2 , U–Pb TIMS) of rutile taken from a ferrodolomite–pyrite–chalcopyrite vein near the Rakkurijärvi area (Martinsson et al., 2016).

3 Methods

3.1 Geologic mapping and sampling

Geologic mapping and structural analysis were carried out between 2019–2021 and during exploration mapping in the early 1990s of the Southeastern Pahtohavare open pit. Approximately 300 field measurements were taken from 130 localities in the field area using Breithaupt Kassel and Silva compasses. Structural measurements are reported using the dip/dip azimuth and plunge/azimuth conventions. For magnetite-rich rocks, sighting measurements guided by known points in the terrain were made with the compass to reduce magnetically induced errors. For the 2019–2021 field campaigns, measurements were digitized directly in the field using the Field Move application (Petroleum Experts Ltd.) on a ruggedized iPad Mini device. Subsequent structural analyses were performed in the software Move (Petroleum Experts Ltd.).

Sampling was conducted in the field and from unoriented drill cores at the Geological Survey of Sweden's National Drill Core Archive in Malå to target structural controls on mineralization. Thirty-seven thin sections were prepared by Precision Petrographics Ltd. in Vancouver, Canada, for petrographic and structural investigation.

3.2 Three-dimensional modeling

The Pahtohavare–Rakkurijärvi area is relatively less explored compared to the central Kiruna area, and the available observations and measurements are concentrated around the closed open-pit areas. The geological model incorporates the structural measurements and the geological map from this study, a digital elevation model based on Lantmäteriet elevation data (2 + m grid precision), and drill hole lithological logs from 31 holes (open-source data from the Geological Survey of Sweden; SGUs Kartvisare, 2022). In total 6625 m of drill cores was available, with an average depth of 214 m. Drill cores were not oriented; therefore structural measurements were not available.

A surface-based modeling approach was applied to build a three-dimensional geological model of the Pahtohavare–Rakkurijärvi area, with the aim to facilitate the visualization and understanding of the lithological and structural framework of the area. The horizontal extent of the model shares the boundaries with the geological map (Fig. 4) and has a vertical range of 1000 m. The vertical range of the model was selected due to the scale of the well-known structures further north in the central Kiruna area and the open end of the structures from the shallow drill holes. A combination of explicit and implicit 3D geomodeling was utilized in Leapfrog Geo (version 2021.2.4, by Seequent). Surface structural measurements were used as implicit, primary indicators for bedding orientations, and the dips were estimated from the continuation of lithological units that were traced through several

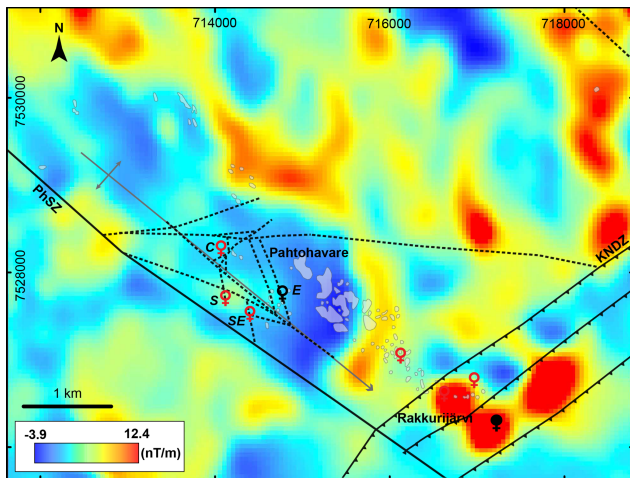


Figure 3. Aeromagnetic anomaly map showing the vertical gradient of the total magnetic intensity anomaly upward continued to 150 m. Symbology as in Fig. 4. Data source: Geological Survey of Sweden (© SGU). Data processing by Thorkild Maack Rasmussen.

drill holes. Contacts of lithological units were implemented explicitly by tracing the lithological boundaries from the geological map and drill hole sections.

4 Results

4.1 Structural analysis

The rocks in the study area are folded into a SE-plunging anticline, which can be visualized in an aeromagnetic anomaly map of the vertical gradient of the total magnetic intensity anomaly (Fig. 3). The rocks are structurally bound to the east and southwest by shear zones trending northeast to southwest and northwest to southeast, respectively (Fig. 3). The NE–SW shear zone forms a part of the Kiruna-Naimakka deformation zone (KNDZ), and the NW–SE shear zone is hereby referred to as the Pahtohavare shear zone (PhSZ; Fig. 3). A summary of the structural mapping results on a geologic map is visualized in Fig. 4, and a full data map can be seen in the Supplement (Fig. S1). Outcrop exposure is approximately 5 % in the field area; however a relatively well-exposed ridgeline runs from the Pahtohavare area parallel to the axial trace of the anticline and flattens into swampy terrain towards the Rakkurijärvi area (Fig. 4). The main formations exposed include a thick horizon of basaltic pillow lavas with minor interlayers of tuffite and chemical sediments and the Kurravaara conglomerate (Fig. 4). A densely exposed and mapped area through these units on the northern limb of the fold is summarized in Fig. 4a. The outcrop exposure on the southern limb of the fold is primarily limited to the open-pit wall of the Southern Pahtohavare deposit (Fig. 4b), which consists of a series of tuffitic and gabbroic units.

The mapping results of the bedding planes collected during the 2019–2021 field campaign and from exploration of the Southeastern deposit during the 1990s are presented in a lower-hemisphere, equal-area stereographic projection (Fig. 4c) and indicate that the geometry of the fold is non-cylindrical, with a subvertical to inclined axial plane, and is SE-plunging ($\beta = 49/161$). In the densely outcropping area in the northern limb of the anticline (Fig. 4a), the bedding orientations appear randomly oriented; however, they show a similar folding orientation in the stereographic projection ($\beta = 19/162$), suggesting parasitic folding occurs. Parasitic folding is also observed in the Southern Pahtohavare open pit (Fig. 5a–b) and in thin sections from the drill core (Fig. 5c–d). The fold axis of one of the parasitic folds (03/090; Fig. 5b) is plotted together with the bedding and cleavage data (Fig. 4c–f) and illustrates that local deviation from the overall orientation of the large-scale fold can occur.

Foliation in the field area often occurs as a bedding-subparallel to bedding-parallel foliation in volcano-sedimentary and sedimentary units. Cleavage mapping data are plotted in Fig. 4d and show an overall similar folding pattern to the bedding, with the fold axis of the foliation occurring steeper than that of the bedding ($\beta = 76/156$). Steeply dipping foliation can be overturned. To account for possible bias from misclassification of bedding versus bedding-subparallel cleavage measurements during mapping, Fig. 4e shows the combined bedding and cleavage measurements, which depict a comparable folding pattern to the bedding data (Fig. 4c) and the map trace of the fold axis (Figs. 3, 4). However, an important observation from this study is the presence of two distinct generations of foliation. The relationship between the two foliations has been observed in rheologically weak units such as tuffites and schists that have been parasitically folded (Fig. 5b) and also in a granitic intrusion approximately 2.5 km southwest of the PhSZ (Fig. 5e). Figure 5b shows the relationship between bedding and foliation in a parasitic fold in the Southern Pahtohavare open pit. The bedding-parallel foliation is defined by biotite and scapolite, and the axial-plane-parallel foliation is spaced and defined by scapolite. The foliation planes have been injected with late scapolite veins. A similar relationship has been observed in the thin section (Fig. 5c–d) from a graphitic schist sample taken from a drill core (full thin-section micrographs can be found in Figs. S2 and S3). This thin section (unoriented) shows folded bedding, bedding-subparallel fabric, and a spaced axial-plane-parallel fabric. The bedding-subparallel fabric is pseudo-mylonitic, with S-C textures (Fig. 5c) and asymmetric porphyroclasts (Fig. 5f) and consistent dextral sense of shear in both limbs of the fold, and suggests non-coaxial strain. The porphyroclasts have recrystallized strain shadows (Fig. 5g–h). The overprinting spaced axial-plane-parallel foliation is defined by fine-grained biotite mineral alignment, as well as by veins of remobilized pyrrhotite–chalcopyrite–pyrite that have utilized S_1 deformation bands (C fabric) for injection.

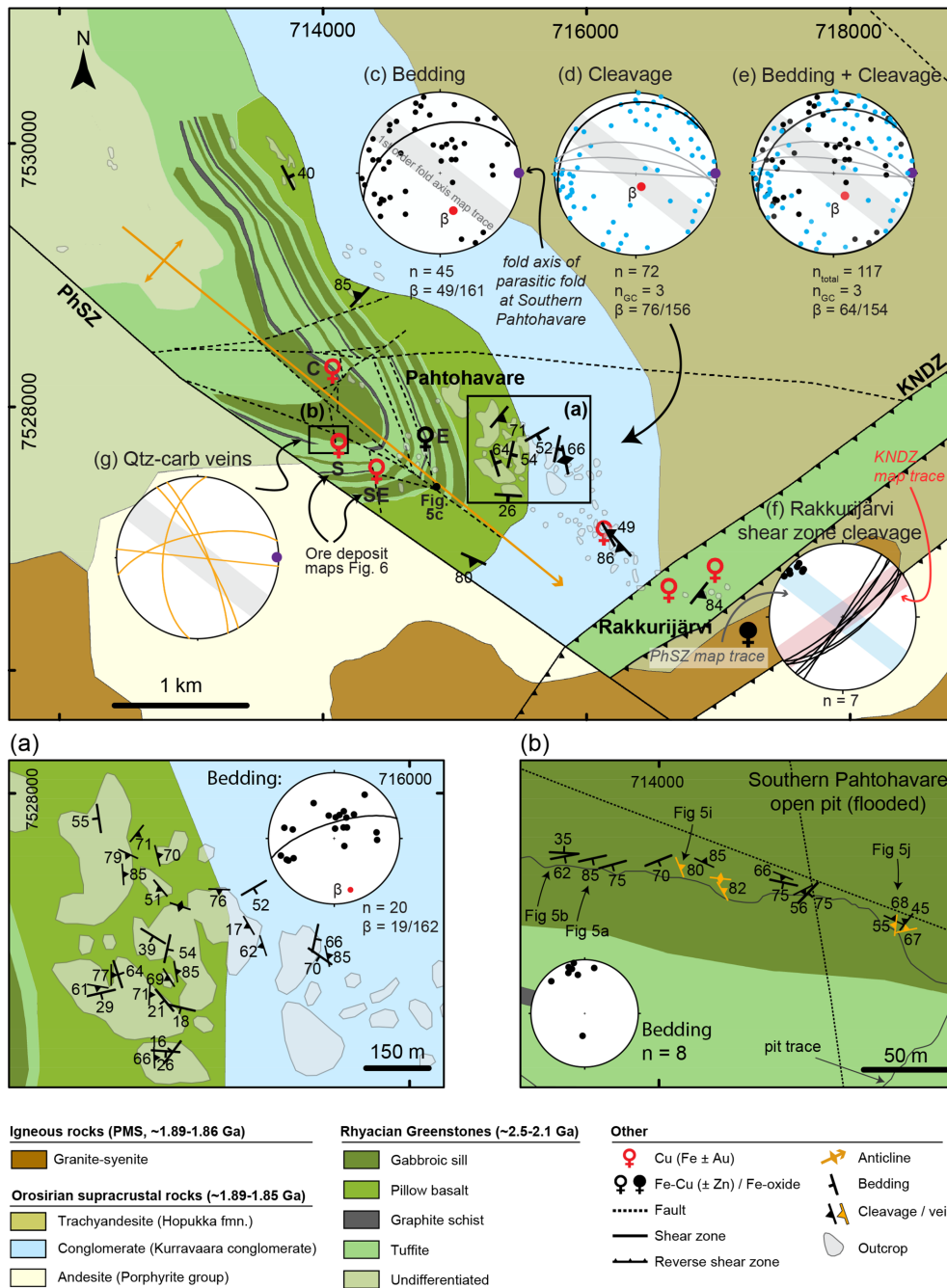


Figure 4. Geologic map of the Pahtohavare and Rakkurijärvi areas with structural results. **(a)** Structural measurements from a densely outcropping area in the northern limb of the anticline. Where multiple measurements existed at the same locality, the visualization was simplified to show the main orientations. A lower-hemisphere, equal-area stereographic projection of bedding planes is shown for this area. **(b)** Structural measurements from the Southern Pahtohavare deposit open pit with a stereographic projection of bedding planes. **(c–e)** Lower-hemisphere, equal-area stereographic projections of all of the structures in the Pahtohavare and Rakkurijärvi area showing bedding **(c)**, cleavage **(d)**, and combined bedding and cleavage **(e)**, respectively. **(f)** Cleavage measurements near the Rakkurijärvi shear zone. **(g)** Quartz-carbonate vein orientations at the Southern Pahtohavare open pit. Gray band shows the apparent fold-axis map trace. Gray great circles (GCs) indicate axis-subparallel veins to the parasitic fold (fold axis: purple dot) at the Southern Pahtohavare open pit. PhSZ: Pahtohavare shear zone; KNDZ: Kiruna-Naimakka deformation zone; S: Southern Pahtohavare deposit; SE: Southeastern Pahtohavare deposit; C: Central Pahtohavare deposit; E: Eastern Pahtohavare deposit. Modified after Martinsson et al. (1993) and Martinsson (1997). Coordinate system in SWEREF99.

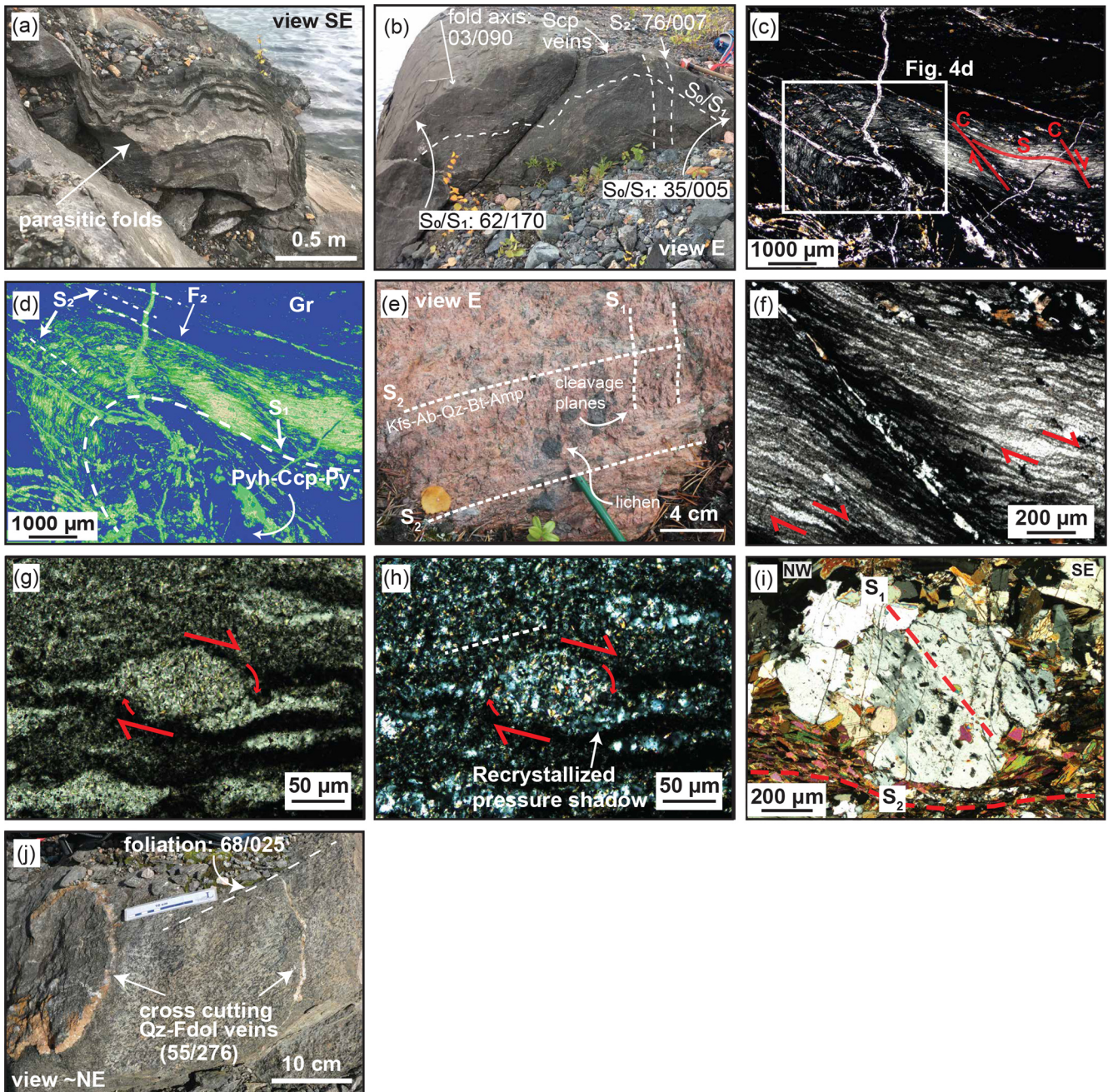


Figure 5. Photographs of structural features in the Pahtohavare–Rakkurijärvi area. (a–b) Parasitic folds in tuffitic layers as a part of a bigger fold system. Photos taken at Southern Pahtohavare open pit. (c) Micrograph of micro-scale fold in graphitic schist from drill core near the Eastern Pahtohavare deposit showing pseudo-mylonitic S-C fabric. Photo in plane-polarized light. Full thin-section micrographs in plane-polarized and reflected light can be found in Figs. S2 and S3. (d) False-color image of graphitic schist in panel (c) highlighting S_1 , S_2 , and F_2 . Remobilized chalcopyrite, pyrite, and pyrrhotite occur in the fold hinge and in the spaced axial planar cleavage. (e) Granitic intrusion 2.5 km southwest of Pahtohavare showing two directions of tectonic cleavage. (f) Plane-polarized light micrograph of the graphite schist in panel (e), showing asymmetric sigmoidal clasts with dextral sense of shear. (g) Plane-polarized light of an asymmetric sigmoidal clast from the graphite schist in panel (e) with recrystallized pressure shadows showing non-coaxial strain, (h) cross-polarized light (XPL) of the same clast, (i) Scapolite porphyroblast showing preserved foliation trails (S_1) and wrapped by a foliation defined by biotite (S_2). (j) Foliated mafic sill with Qz–Fdol veins cross-cutting at a high angle at the Southern Pahtohavare open pit. Structural measurements: dip/dip azimuth. Scp: scapolite; Gr: graphite; Pyh: pyrrhotite; Ccp: chalcopyrite; Py: pyrite; Kfs: K-feldspar; Ab: albite; Qz: quartz; Bt: biotite; Amp: amphibole; Fdol: ferrodolomite.

An additional example of two distinct fabrics is shown in an oriented thin section from a shear zone in the Southern Pahtohavare open pit by preserved foliation trails in a scapolite porphyroblast which are discordant to the foliation that wraps around it (Fig. 5i). The combined structural, outcrop, and thin-section observations indicate the fold in the Pahtohavare–Rakkurijärvi area is an F_2 fold formed under non-coaxial strain and that both S_1 and S_2 fabrics are preserved.

The NE–SW-trending KNDZ near the Rakkurijärvi area causes a transposition of the foliation direction into a NE–SW orientation that quickly dissipates in outcrops away from the shear zone boundary (Fig. 4f). Tensional gashes and brittle fracturing record tensile openings with a NW–SE orientation directly in the shear zone. The NW–SE-trending PhSZ was mapped via small-scale (10–15 cm wide) shear zones from the Southern Pahtohavare open pit. One quartz–carbonate ± pyrite ± chalcopyrite shear band with the orientation 80/065 indicates the shear zone is steeply dipping, and a mineral lineation defined by scapolite (55/162) on the foliation plane shows that oblique–reverse movement characterizes the sense of shear.

A new mine level map from the 300 m level at the Southern Pahtohavare deposit is presented in Fig. 6a. The lithological contacts and the structures presented on the map were interpolated using vertical cross-sections from three to five inclined drill holes every 10 m along-strike of the ore body. The geometry of the ore body indicates the mineralization is strongly structurally controlled by undulating WNW- to NW-directed shear zones as well as by secondary brittle faults. Importantly, at the surface at Southern Pahtohavare open pit, quartz–carbonate ± pyrite ± chalcopyrite shear bands and veins, a main ore-related mineral assemblage for the epigenetic Pahtohavare deposits, are observed cross-cutting tectonic cleavage (Figs. 4g, 5j). These veins occur as both brittle fractures and ductile shear zones at orientations close to parallel or at an angle to the axial plane of the fold (Fig. 4g). Similarly, at the Southeastern deposit (Fig. 6b), a discordant ore zone trends north-northwest–south-southeast in an off-axis orientation to the axial plane of the fold. The discordant ore zone cuts the bedding in the tuffite and the gabbroic sill at a high angle and splits into lower-order structures towards the stratabound portion of the deposit.

4.2 Geological model

A 3D geological model generated based on drill hole data and the geological map (Fig. 4) visualizes the main lithological boundaries and structures for the study area (Fig. 7). The relatively shallow drill holes (down to 300 m) indicate a complex intercalation between gabbro, graphitic schist, hornblende, chert, and greenstones composed mainly of basaltic tuff. Based on the lithological logs from the drill cores, the markers were grouped into four units: graphite schist,

gabbroic sill, pillow basalts, and undifferentiated greenstones. The trachyandesitic Hopukka formation, andesitic Porphyrite group, igneous granite–syenite of the PMS, and the Kurravaara conglomerate were not intersected by the selected drill holes and were traced based on the map extent to constrain the model. Faults were added based on the geological map (illustrated in red in Fig. 7) and were modeled as hard boundaries that separate fault blocks. Two perpendicular conceptual cross-sections were created based on the geological model (AA' and BB' in Fig. 7) and contain additional interpretations for an improved visualization of the crustal architecture, illustrating the SE-plunging anticline and the relationship between the lithostratigraphic units. The conceptual cross-sections highlight the geometry of the fold, showing a curvilinear fold axis and a plunge to the southeast (AA' in Fig. 7a) and the anticlinal nature with a subvertical axial plane which trends subparallel to the NW–SE PhSZ (BB' in Fig. 7b). Furthermore, it illustrates the interplay between the major shear zones and secondary fault structures that show minimal offset but are interpreted to have formed as a result of brittle–plastic, non-coaxial strain between the two conjoining shear zones. The NW–SE-oriented PhSZ truncates the southwestern limb of the Pahtohavare fold and probably played an important role in controlling the shape of the fold during the deformational events.

5 Discussion

Clarifying the timing of Cu–Au mineralization and the tectonic regime during emplacement is critical for understanding the mineral systems and the relationships between IOA and IOCG deposits in Norrbotten. However, the overprinting deformation, metamorphic, magmatic, and alteration events associated with the Svecokarelian orogeny complicate interpretation of the vectors to the ore and the identification of ingredients of the different mineral systems. Some Cu–Au mineralization in Norrbotten has been linked to the early-Svecokarelian orogeny (e.g., Aitik porphyry Cu (Au–Ag–Mo) deposit, see Fig. 1; Rakkurijärvi IOCG, see Fig. 2; Wanhainen et al., 2012; Smith et al., 2007), but a significant contribution of Cu–Au occurs as late-orogenic overprints (e.g., IOCG overprint at Aitik and the Nautanen deformation zone as well as at the Malmberget and Gruvberget IOA deposits; Fig. 1; Wanhainen et al., 2012; Martinsen et al., 2016; Bauer et al., 2018, 2022). Therefore, assessing energy drivers (e.g., magmatism, deformation), fluid and metal sources, transport pathways, and traps (Wyborn et al., 1994) by framing them within the tectonic framework is useful for unraveling complicated and overprinted relationships. The question of which mineralized deposits are associated with each tectonic phase of the Svecokarelian orogeny (early or late) and whether these represent unique mineralization events remains an important factor in understanding what genetic connection IOA and IOCG deposits share. Be-

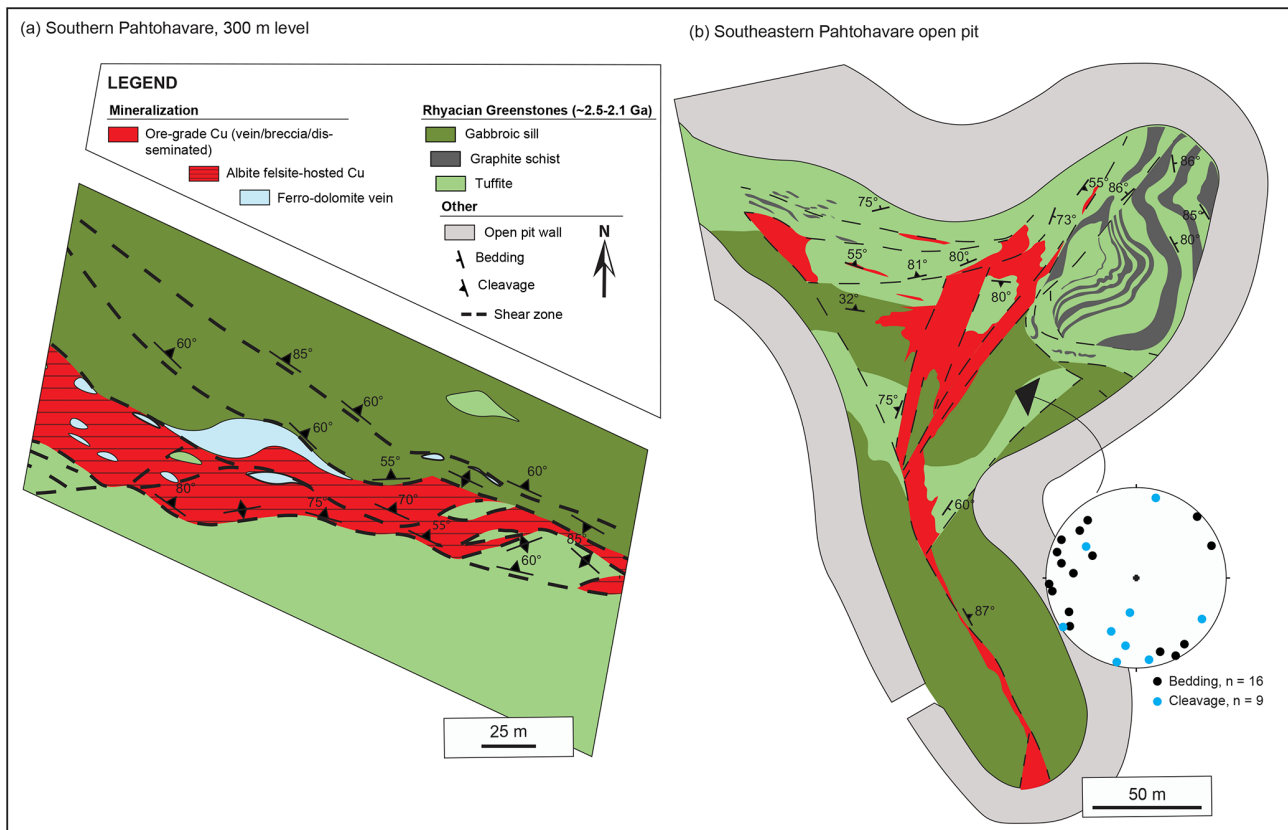


Figure 6. (a) A mine level map at 300 m of the Southern Pahtohavare deposit showing albite-felsite-hosted Cu in a structurally controlled position. The construction of the mine level map was done for resource estimates during the 1990s by utilizing vertical cross-sections from profiles every 10 m along the strike of the ore body, with three to five inclined drill holes in each profile intersecting the ore body at various depths. Geological contacts and structures have been interpolated from the vertical cross-sections. Dipping of contacts and structures is estimated from the cross-sections and is not based on actual structural measurements. (b) The Southeastern Pahtohavare open pit showing both the stratabound and discordant ore zones. Structural measurements were acquired during mapping in the 1990s.

low, the structural context and relative timing of the Pahtohavare epigenetic deposits are discussed and temporally placed within the context of the tectonic framework. Additionally, the structural setting for transport pathways and traps of the mineral systems of the Kiruna mining district is discussed.

5.1 Structural context and timing of ore-forming processes for the Pahtohavare epigenetic deposits

The structural characterization of the northern Norrbotten ore province defines two major periods of fabric development during the Svecokarelian orogeny. Regionally, S_1 reflects an inferred NE–SW crustal shortening which formed a regionally distributed and penetrative, yet heterogeneously developed fabric (Bergman et al., 2001; Grigull et al., 2018; Bauer et al., 2018; Andersson et al., 2020; Bauer et al., 2022). S_2 records an inferred E–W crustal shortening forming a spaced fabric (Luth et al., 2018b; Grigull et al., 2018; Bauer et al., 2018, 2022; Andersson et al., 2020, 2021). The structural results from this study show that two dis-

tinct fabrics are preserved in the Rhyacian greenstones and lower Orosirian rocks in the Pahtohavare–Rakkurijärvi area. An early S_1 fabric occurs bedding-subparallel in volcano-sedimentary and sedimentary rocks and is interpreted to be tectonically formed from non-coaxial strain based on microstructural observations of mylonitic textures and asymmetric sigmoidal clasts with recrystallized pressure shadows (Fig. 5c, f, g–h). Additionally, preserved foliation trails in a scapolite porphyroblast taken from the Southern Pahtohavare open pit show an early tectonic fabric is preserved (Fig. 5i). A late S_2 fabric is observed occurring axial-plane-parallel to folded bedding + S_1 foliation (Figs. 5c, S2–S3). The fabric is spaced, suggesting brittle–plastic conditions, which agrees with the described nature of the late-Svecokarelian deformation event (Luth et al., 2018b; Grigull et al., 2018; Andersson et al., 2020; Bauer et al., 2022). Despite two fabrics being identified microstructurally, field evidence unfortunately provided few clear outcrops showing the relationship between the two foliations. However, it is observed in parasitic folding from the Southern Pahtohavare open pit (Fig. 5a–b), which

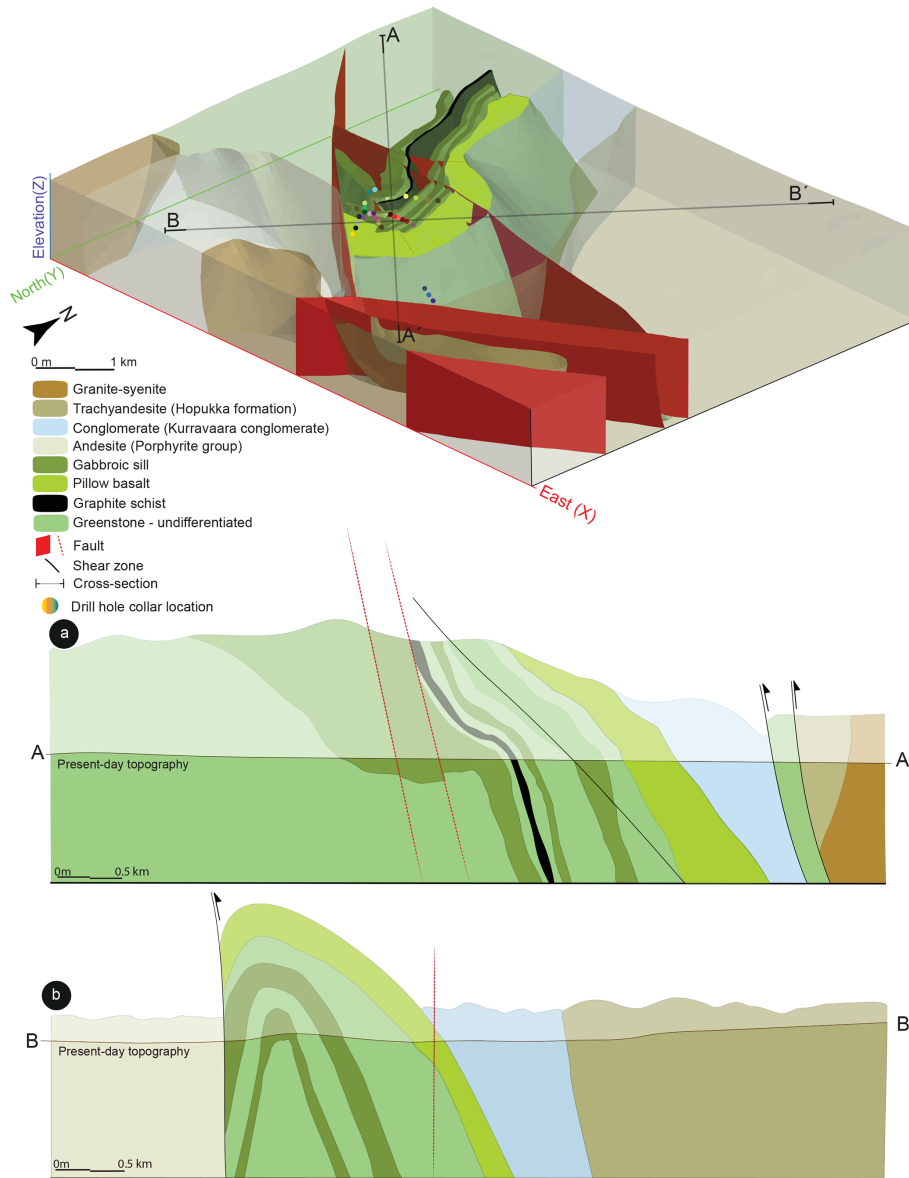


Figure 7. Local 3D model (viewed from above and towards the northwest) and conceptual cross-sections of the southern Kiruna mining district showing the major lithological boundaries, faults, and shear zones. The geological 3D model is built based on the local geological map, structural measurements, and lithological drill hole logs (drill hole numbers and coordinates can be found in Supplement Table S1). The 3D model highlights the Pahtohavare F_2 fold by utilizing different transparency levels of the adjacent lithological units. The conceptual cross-sections interpreted from the 3D model and structural data in this study highlight the geometry of the fold and the relationship between brittle–ductile structures and local lithostratigraphic units from a (a) NW–SE orientation and (b) SW–NE orientation. An interactive 3D model is available in Fig. S4.

also shows bedding-subparallel foliation and spaced axial-plane-parallel S_2 foliation. The foliation planes portrayed in the stereographic projections (Fig. 4d) therefore were not divided into early versus late generations owing to the lack of field relationships. However, the summary of all the cleavage data (Fig. 4d) maintains a relatively consistent fold pattern to the bedding. We presume the S_2 foliation present in the

dataset trends subparallel with the fold axis of the fold in the Pahtohavare area.

The bedding data (Fig. 4c) agree with the first-order map trace of the fold observed in the aeromagnetic anomaly map (Fig. 3). Furthermore, the data show that the fold is noncylindrical and suggest that the plunge of the fold can vary between steep and shallow. This is observed from the data plotted from the northern limb (Fig. 4a), which shows a mod-

erately shallow dip compared to the overall plunge of the fold from the bedding data, which is steeper (Fig. 4c). Additionally, the parasitic fold measured from the Southern Pahtohavare open pit (Fig. 5b) has a near-horizontal fold axis (03/090). Therefore, our conceptual interpretation of this feature (Fig. 7a) shows a fold plunging to the southeast that has a curvilinear fold axis. Parasitic folding is observed in both drill cores (Fig. 5c) and outcrops (Fig. 5a–b) and can be deduced from the mapping measurements in the field (Fig. 4a). While the single measurement of the fold axis of the parasitic fold deviates from the main orientation of the fold in the area (Figs. 4c, 5b), this could be explained by deflection or transposition during folding and/or shearing. Further evidence that the parasitic folds are associated with the SE-plunging anticline is the apparent random orientations of bedding planes in the northern limb that, when plotted into a stereographic projection, show a similar fold-axis plunge direction, arguing for a coaxial relationship (Fig. 4a). Together, the bedding and cleavage results strongly indicate that the anticline in the Pahtohavare–Rakkurijärvi area is an F_2 fold formed during the late-Svecokarelian orogeny.

Kinematic information on the PhSZ has not previously been described with structural data. The results in this study show that the shear zone is steeply dipping to the northeast (80/065) based on data from local small-scale (10–20 cm wide) shear zones in the Southern open pit. In the shear bands, quartz–ferrodolomite–calcite–pyrite–chalcopyrite mineral assemblages are boudinaged and infiltrate along folded bedding planes which reflect plastic behavior during syn-tectonic emplacement, likely coeval to the folding. A scapolite mineral lineation on a foliation plane within the shear zone indicates movement with the orientation 55/162. Forming the anticlinal fold from E–W crustal shortening during the late Svecokarelian requires the movement along the shear zone to have been dominantly reverse with a minor sinistral component as opposed to a normal–dextral movement.

The Southern and Southeastern Pahtohavare deposits are both strongly structurally controlled (Fig. 6). A WNW- to NW-oriented structure shears the Southern deposit (Fig. 6a), forming steep shear contacts between the ore and the host rocks. Similarly, at the Southeastern deposit, a subvertical NNW-oriented shear structure controls the discordant ore zone, which cuts the hosting mafic sill and the bedding in the tuffite at a high angle (Fig. 6b). The orientation of these features forms either an axial-plane-parallel orientation to the Pahtohavare fold (Southern) or an acute angle to the PhSZ (Southeastern) and likely represents secondary brittle–ductile faults formed in response to reverse–oblique shearing along the shear zone during the late-Svecokarelian orogeny. The orientations of the quartz–carbonate veins from the Southern Pahtohavare open pit show either a N–S to NNW–SSE or an E–W orientation (Fig. 4g), which supports the notion that lower-order structures play a role in the mineralization. The quartz–carbonate veins also cross-cut tectonic

foliation (Fig. 5j) in the Southern Pahtohavare open pit, indicating a late-Svecokarelian orogenic timing for emplacement.

In the absence of a regional tectonic framework and geochronological constraints, the timing of the epigenetic Pahtohavare deposits was unknown but has been suggested to be of similar age to the Rakkurijärvi IOCG deposit, for which radiometric age data (Re–Os molybdenite, U–Pb LA-ICP-MS allanite, U–Pb TIMS rutile) indicate formation at ca. 1.86 Ga (Smith et al., 2007, 2009; Martinsson et al., 2016). However, the results of this structural investigation and the designation of the Pahtohavare fold as F_2 allow the Pahtohavare epigenetic deposits to be assigned to the late-Svecokarelian mineral system, which in Kiruna is constrained by syn-tectonic titanite data at ca. 1.81–1.79 Ga (Andersson et al., 2022). Furthermore, this illustrates that brittle–ductile, non-coaxial shear zones and resultant S_2 and lower-order structures associated with the E–W-oriented late-orogenic deformation served as pathways for ore fluids. In the Pahtohavare area, traps for the mineral system likely occur where these pathways intersect favorable reducing horizons of graphitic schist, which is the main lithological trap for the ore (Martinsson et al., 1997a). The structural results from this study are the first to show a late-Svecokarelian timing for Cu ± Au mineralization in the Kiruna mining district.

5.2 Structural framework in Kiruna

A conflicting result from this study that complicates the interpretation of how the regional tectonic evolution is expressed in the Kiruna mining district is the preserved S_1 foliation in the Rhyacian greenstone rocks (Kiruna greenstone group) and lower Orosirian rocks (Kurravaara conglomerate), which is absent or masked in the overlying Orosirian rocks (Andersson et al., 2021). While an S_1 fabric is observed regionally (Bergman et al., 2001; Grigull et al., 2018; Bauer et al., 2018; Andersson et al., 2020; Bauer et al., 2022), the lack of an S_1 fabric in the central Kiruna area was suggested to indicate that the rocks were at a higher crustal level and did not experience plastic deformation during the early-orogenic phase. Furthermore, to the west and southeast of Kiruna structural evidence shows that blocks of lower crustal levels (and subsequently higher metamorphic grades) were uplifted with reverse west-side-up kinematics along steep W-dipping structures (Bergman et al., 2001; Andersson et al., 2020), and to the east and northeast, reverse east-side-up kinematics occur along E-dipping structures (Luth et al., 2018b; Andersson et al., 2021). Other structural investigations have noted that the Kiruna area records fewer folding phases compared to the regions to the north and east (Vollmer et al., 1984; Grigull et al., 2018; Luth et al., 2018b). A bedding-parallel S_0 compaction fabric is described for the Orosirian sequence in the central Kiruna area; however, the mylonitic bedding-subparallel fabric observed in the thin section (Fig. 5c–d),

the S_1 foliation trails in a scapolite porphyroblast (Fig. 5i), and the two generations of tectonic fabric in granitic intrusions in the southern part of the district (Fig. 5e) rule out that the foliation in these areas is a result of compaction alone. Evidence of S_1 (or S_0/S_1) and S_2 fabrics is also noted in a previous mapping campaign in the Saarijärvi area (Martinsson et al., 1993). Two possible explanations for this discrepancy are that the S_1 fabric developed heterogeneously in response to shearing and/or to an elevated geothermal gradient. Relatively localized shearing could account for the heterogeneously developed tectonic fabric found in the greenstone sequence (e.g., graphite schists, pyroclastic tuffs, mafic sills; e.g., Fig. 5b–c, j). However, ductile deformation could also have occurred due to a locally elevated geothermal gradient in this area. Logan et al. (2022) recently conducted U–Pb zircon geochronology on several intrusions in the southern part of the district that showed a dominantly early-Svecokarelian timing for the magmatism. The abundant magmatism would have resulted in increased fluid circulation and may have facilitated the heterogenous formation of a ductile S_1 fabric. Extensive hydrothermal fluid flow driven by abundant igneous activity has been postulated as an explanation for the regional-style Na metasomatism (e.g., scapolite and albite), which is also restricted to large-scale shear zones (Frietsch et al., 1997; Bergman et al., 2001). In the central Kiruna area the regional-style scapolite alteration occurs more rarely (Bergman et al., 2001; Martinsson, 2004), and the Na–Ca (+ Fe ± Cl) and alkali alteration styles recorded are spatially associated with local IOA deposits (Martinsson, 2015; Martinsson et al., 2016).

A conceptual framework of the structural evolution of the Kiruna area is proposed in Fig. 8, which synthesizes the structural results presented in this paper with those produced by Andersson et al. (2021) and is also based on previous structural mapping from the Kiruna area (Wright, 1988; Martinsson et al., 1993; Grigull et al., 2018) as well as the Geological Survey of Sweden's magnetic anomaly map of the district (Fig. 3; Bergman et al., 2001). This framework is offered as a working model and can be subject to modification with future work in the district. The NW–SE-trending PhSZ to the southwest of the fold in the Pahtohavare–Rakkurijärvi area is interpreted to be a reactivated early normal fault structure. This structure formed during the back-arc extension of the early-Svecokarelian orogeny (Fig. 8a) or possibly even earlier, during the Rhyacian rifting. Upon the early NE–SW-oriented crustal shortening at ca. 1.87 Ga (Fig. 8b), the structure reactivated with reverse kinematics, and an early tectonic S_1 fabric was heterogeneously developed, possibly forming as a shear foliation and/or as a result of a locally elevated geothermal gradient. At the same time, the NE–SW to N–S KNDZ that runs adjacent to the Rakkurijärvi deposit and through central Kiruna (Figs. 2–4) would have responded with oblique–reverse shearing (Fig. 8b) and offered conduits along which ore fluids could be transported. During the E–W brittle–plastic crustal shortening of the late-

Svecokarelian orogeny, extensive reactivation of fault systems occurred in the Kiruna mining district (Fig. 8c). Basin inversion manifested from the crustal shortening (Andersson et al., 2021), and strong strain partitioning occurred, forming high-strain fabrics along shear zones and spaced to heterogeneously developed fabric outside of these zones. Conjugate faulting subparallel to the E–W shortening direction occurred in response to the stress direction (Fig. 8c). The PhSZ responded with reverse–oblique (sinistral) kinematics, causing vertical extrusion of the rocks and noncylindrical anticlinal folding (Figs. 7, 9). This juxtaposed the older Rhyacian volcanic rocks to the northeast with younger Orosirian volcanic rocks to the southwest (Figs. 4, 9). During this time the brittle–ductile strain created tensional structures for ore fluids to propagate through in the Pahtohavare area. Finally, at ca. <1.79 Ga (see Andersson et al., 2022), a N–S-oriented crustal shortening led to gentle refolding (Andersson et al., 2021) and minor reactivation of preexisting fault structures (Fig. 8d).

5.3 Implications for the Kiruna mining district mineral systems and relationships between IOA and IOCG mineralization

This study shows that multiple mineralization events in the Kiruna mining district can be linked to specific phases of the tectonic evolution. Using the proposed structural framework presented in Fig. 8, the timing of mineralization within a structural context can be synthesized. The earliest mineralization known in the district (e.g., Viscaria and Eastern Pahtohavare; Fig. 2) has been suggested to have occurred syngenetically during deposition of the Kiruna greenstone group around ca. 2.1 Ga from Rhyacian rifting (Martinsson et al., 1997a, b). Following this mineralization and rifting period, during the Orosirian back-arc extension and basin development in the district, the development of syn-volcanic normal and transtensional faults (Fig. 8a) occurred around 1889 ± 26 Ma (Andersson et al., 2022), shown by in situ U–Pb (LA-ICP-MS) dating of titanite in a hydrothermally altered damage zone to a fault system associated with the Luosavaara IOA deposit. Such a timing is coeval with volcanism in the district as well as the accepted age for the IOA formation (1888 ± 6 Ma: U–Pb ICP-MS titanite; 1874 ± 7 and 1877 ± 4 Ma: U–Pb SIMS zircon; 1878 ± 4 Ma: U–Pb TIMS titanite; Romer et al., 1994; Westhues et al., 2016; Martinsson et al., 2016). It was therefore suggested that normal faulting in an extensional regime may have played an important role for the emplacement of the IOA ore (Andersson et al., 2022). Conversely, following the onset of crustal shortening (Fig. 8b), the Rakkurijärvi IOCG deposit formed and is described to be related to the NE–SW shear zone (KNDZ) adjacent to the deposit (Smith et al., 2007), implying that the faulting was active around ore formation at ca. 1.86 Ga (Smith et al., 2007, 2009; Martinsson et al., 2016). Such a context supports the notion that IOA and IOCG deposits may

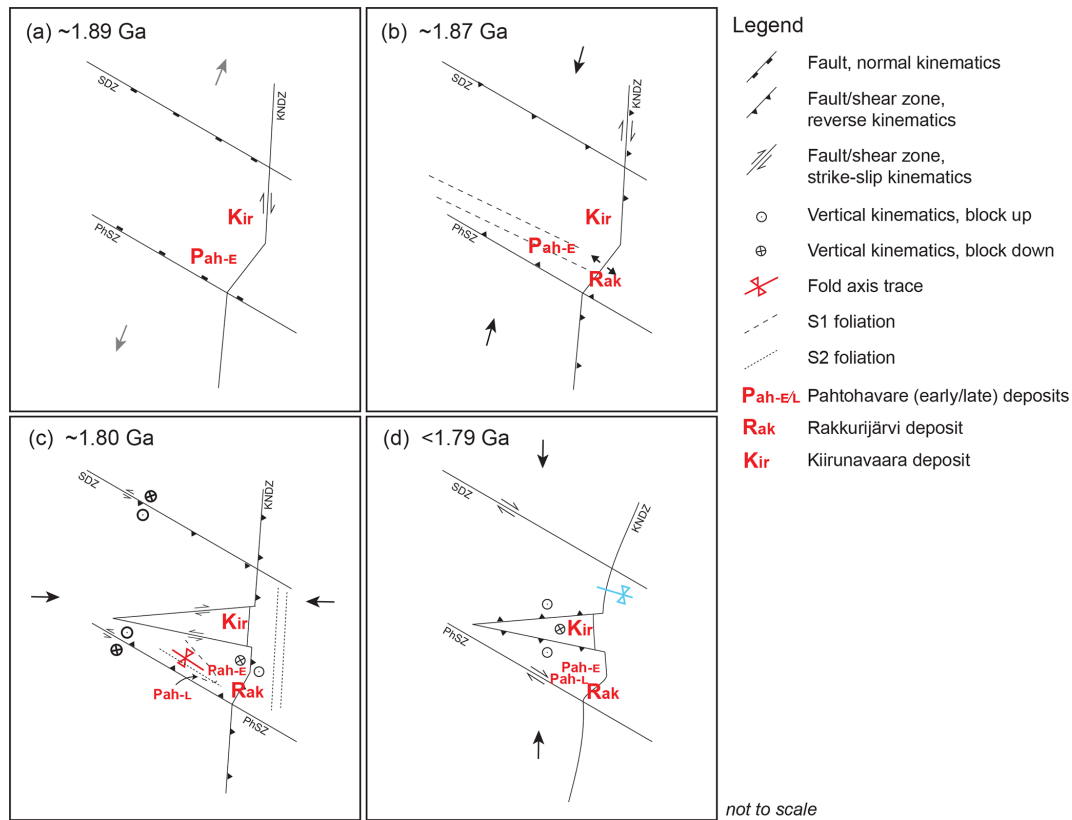


Figure 8. A proposal for the structural framework for the Kiruna mining district. **(a)** The onset of the Svecofennian orogeny and back-arc extension forms and/or reutilizes preexisting normal faults, and additional transtensional faults form. The earliest (ca. 2.1 Ga) Pahtohavare syngenetic deposit (Eastern, Pah_E) has already formed, and the Kiruna IOA deposit forms. **(b)** NE–SW crustal shortening from the early-Svecofennian orogeny reactivates preexisting fault structures, forming transpressional shear zones and dilatational jogs. The Rakkurijärvi IOCG forms (Rak). Early S₁ fabric develops in the southern Kiruna mining district. **(c)** Late-orogenic E–W crustal shortening and basin inversion occur. Stratigraphy in the Pahtohavare–Rakkurijärvi area is folded, and S₂ foliation develops. Strong strain partitioning occurs, with S₂ fabric forming along shear zones in the central Kiruna area. Both brittle and ductile structures form. The late epigenetic Pahtohavare deposits form (Pah_L). **(d)** N–S crustal shortening causes gentle refolding in the district, and minor reactivation of preexisting structures occurs. SDZ: Svappavaara deformation zone; KNDZ: Kiruna-Naimakka deformation zone; PhSZ: Pahtohavare shear zone.

form within 20 Myr of each other, as indicated in other classic IOCG–IOA terrains (e.g., the Chilean iron belt; see Skirrow, 2021, and references therein). It is possible that IOA and IOCG deposits share some mineral system ingredients; however, in Kiruna distinct tectonic regimes separate the formation of IOA and IOCG deposits, respectively (Fig. 8a–c).

The establishment of a late-orogenic timing for the epigenetic Pahtohavare Cu ± Au deposits indicates that a time gap of ca. 80 Myr or more exists between the younger episode of Cu ± Au mineralization and the IOA emplacement in the Kiruna mining district. The indicated time gap introduces important implications for the current debates about IOA and IOCG genetic continuums (see Reich et al., 2016; Corriveau et al., 2016; Barra et al., 2017; Simon et al., 2018) as the later Cu ± Au event in Norrbotten lacks clear temporal associations with IOA deposits; this is in line with the mineralization in the Cloncurry district in Australia, where IOCG-style deposits occur without Kiruna-type IOA deposits (see Groves

et al., 2010; Reich et al., 2022). Furthermore, in the Gällivare area, approximately 70 km southeast of Kiruna (see Fig. 1), two distinct mineralizing periods related to different phases of the tectonic evolution are also described. The Malmberget IOA deposit is considered to have formed during the early-orogenic phase (ca. 1.89–1.88 Ga), constrained by the age of the host rocks (Sarlus et al., 2020) and from structural analysis showing the iron ore was affected by two deformation events (Bergman et al., 2001; Bauer et al., 2018). Late IOCG-style mineralization is suggested to have overprinted the area around 1.80 Ga at Aitik (Wanhainen et al., 2012) as well as in the Nautanen deformation zone, where mineralization is also situated in late-orogenic structures (Bauer et al., 2022). From a mineral systems perspective, multiply reactivated structures (e.g., Fig. 8) may play an important role for fluid and transport pathways even if IOA- and IOCG-style mineralization can be separated in time and by tectonic regimes. For example, the N–S- to NE–SW-trending structure adja-

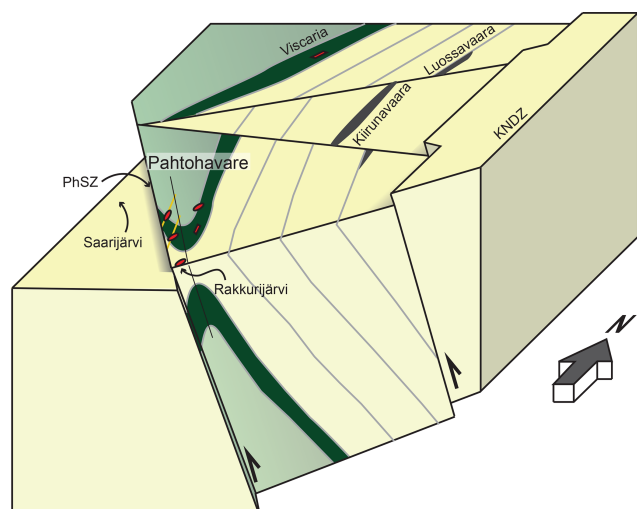


Figure 9. Three-dimensional conceptual model of the Pahtohavare area in the southern Kiruna mining district showing the oblique-reverse NW-SE-trending Pahtohavare shear zone and the resultant Pahtohavare F_2 fold. The axial surface is steeply dipping, and the Pahtohavare epigenetic deposits are controlled by D_2 structures. Green colors denote older greenstone stratigraphy (ca. >2.1 Ga), and yellow colors denote ca. 1.92 Ga and younger stratigraphy. KNDZ: Kiruna-Naimakka deformation zone; PhSZ: Pahtohavare shear zone.

cent to the shear-zone-controlled Rakkurijärvi IOCG deposit (Figs. 2–4) can be constrained by radiometric age determinations (ca. 1.86 Ga; Smith et al., 2007, 2009; Martinsson et al., 2016) but has also been shown by structural analysis to be active during the late-Svecokarelian orogeny (ca. 1.81–1.79 Ga; Andersson et al., 2021, 2022). Furthermore, U–Pb (SC-ICP-MS) ages from monazite in hydrothermal calcite found within the same shear zone in central Kiruna show that the structure was again active at ca. 1.78–1.76 Ga (Lauri et al., 2022). The point that these reactivated transport pathways facilitated overprinting alterations and mineralization emphasizes the importance of incorporating the tectonic framework into the assessment of these complex mineral systems.

6 Conclusion

The northern Norrbotten ore province has a complex tectonic evolution and mineralization history and requires mineral systems assessments to be made utilizing a regional tectonic framework. The Pahtohavare–Rakkurijärvi area in the southern Kiruna mining district hosts syngenetic and epigenetic Cu ± Au and IOCG mineral occurrences which have not been structurally contextualized within the tectonic evolution of the region. In the Pahtohavare–Rakkurijärvi area, the Rhyacian to lower Orosirian volcanic, volcanoclastic, and sedimentary bedrock is anticlinally folded and bound by two shear zones trending northwest to southeast on the south-

western limb and northeast to southwest to the east. New structural data show that the fold is noncylindrical and has a subvertical to steeply inclined axial plane, with a fold axis plunging to the southeast, in agreement with previous work. Bedding-subparallel foliation shows an accordant folding pattern, and structural analysis from thin section shows that the foliation is mylonitic and has porphyroclasts with pressure shadows, supporting a tectonic origin for the S_1 fabric. The data constrain the fold in the Pahtohavare–Rakkurijärvi area as F_2 with folded S_1 foliation and axial-plane-parallel S_2 foliation developed. Importantly, the epigenetic Cu ± Au Pahtohavare deposits are strongly structurally controlled, and quartz–carbonate–sulfide vein generations are observed to be cutting foliation, trending axial-plane-parallel, and at an angle to the F_2 Pahtohavare fold-axis trace, structurally constraining the deposits to the late-orogenic phase of the Svecokarelian orogeny. These results mark the first time a deposit in the Kiruna mining district has been linked to the late phase of the orogeny. The shear zones binding the fold in the Pahtohavare–Rakkurijärvi area are interpreted to be reactivated early structures, and oblique-reverse kinematics are proposed for the NW-SE shear zone to explain the geometry of the fold in response to E–W crustal shortening. A time gap of ~80 Myr between the formation of the Kiirunavaara IOA deposit and the formation of the Pahtohavare epigenetic Cu ± Au deposits holds important implications about the timing of iron oxide (apatite) and copper–gold precipitation in Kiruna, showing that at least two distinct mineralizing periods can be constrained to different phases of the tectonic evolution.

Data availability. Aeromagnetic anomaly and outcrop locality data were obtained from the Geological Survey of Sweden (<https://maps.slu.se/>, Geological Survey of Sweden, 2019). The digital elevation map used for the 3D model is from Lantmäteriet (Lantmäteriet, 2015; <https://www.lantmateriet.se/sv/geodata/vara-produkter/produktlista/markhojdmodell-nedladdning/>). Drill hole logs used for the 3D model were obtained from the SGU open-source map viewer (<https://apps.sgu.se/kartvisare/>; SGUs Kartvisare, 2022). All geologic maps used in this work are cited in the main text and reference sections. Structural field measurements collected during the field seasons are presented in the Results section, in Figs. 4 and 6, and in Supplement Fig. S1 and are available from the corresponding author.

Supplement. The supplement related to this article is available online at: <https://doi.org/10.5194/se-14-763-2023-supplement>.

Author contributions. LL conducted the geological mapping, processed the structural data, sampled and conducted thin-section petrography, visualized the results, wrote the original manuscript, and reviewed and edited the final manuscript. EV made the 3D geologic model from drill logs, visualized the results, wrote sections

of the original manuscript, and edited the final manuscript. JBHA assisted with fieldwork and structural interpretations, visualized the mine maps, and edited the final manuscript. OM conducted geologic mapping, drew the original mine maps, assisted with structural interpretations, and edited the final manuscript. TEB secured funding, supervised, assisted with fieldwork and structural interpretations, visualized the results, and edited the final manuscript.

Competing interests. The contact author has declared that none of the authors has any competing interests.

Disclaimer. Publisher's note: Copernicus Publications remains neutral with regard to jurisdictional claims in published maps and institutional affiliations.

Acknowledgements. This work is part of the European Union's Horizon 2020 project "New Exploration Technologies – NEXT". Lovisagruvan AB and Critical Metals Scandinavia AB are thanked for providing access to open pits. Petroleum Experts Ltd. is thanked for donating the MOVE 2017 software. The staff at the Geological Survey of Sweden is thanked for their help and collaboration during sampling at the National Drill Core Archive in Malå, Sweden. Thorkild Rasmussen is thanked for reducing the aeromagnetic anomaly data. The constructive input from Pietari Skyttä and Giovanni Musumeci greatly improved the paper, and they are thanked for their reviews.

Financial support. This research has been supported by the Horizon 2020 research and innovation program (grant no. 776804).

Review statement. This paper was edited by Virginia Toy and reviewed by Pietari Skyttä and Giovanni Musumeci.

References

- Andersson, J. B. H., Bauer, T. E., and Lynch, E. P.: Evolution of structures and hydrothermal alteration in a Palaeoproterozoic supracrustal belt: Constraining paired deformation–fluid flow events in an Fe and Cu–Au prospective terrain in northern Sweden, *Solid Earth*, 11, 547–578, <https://doi.org/10.5194/se-11-547-2020>, 2020.
- Andersson, J. B. H., Bauer, T. E., and Martinsson, O.: Structural Evolution of the Central Kiruna Area, Northern Norrbotten, Sweden: Implications on the Geologic Setting Generating Iron Oxide-Apatite and Epigenetic Iron and Copper Sulfides, *Econ. Geol.*, 116, 1981–2009, <https://doi.org/10.5382/econgeo.4844>, 2021.
- Andersson, J. B. H., Logan, L., Martinsson, O., Chew, D., Kooijman, E., Kielman-Schmitt, M., Kampmann, T. C., and Bauer, T. E.: U-Pb zircon-titanite-apatite age constraints on basin development and basin inversion in the Kiruna mining district, Sweden, *Precambrian Res.*, 372, 106613, <https://doi.org/10.1016/j.precamres.2022.106613>, 2022.
- BABEL Working Group: Evidence for early Proterozoic plate tectonics from seismic reflection profiles in the Baltic shield, *Nature*, 348, 34–38, <https://doi.org/10.1038/348034a0>, 1990.
- Barra, F., Reich, M., Selby, D., Rojas, P., Simon, A., Salazar, E., and Palma, G.: Unraveling the origin of the Andean IOCG clan: A Re-Os isotope approach, *Ore Geol. Rev.*, 81, 62–78, <https://doi.org/10.1016/j.oregeorev.2016.10.016>, 2017.
- Barton, M. D.: Iron Oxide–Cu–Au–REE–P–Ag–U–Co) Systems, in: *Treatise on Geochemistry*, Elsevier, 515–541, <https://doi.org/10.1016/B978-0-08-095975-7.01123-2>, 2014.
- Bauer, T. E. and Andersson, J. B. H.: Structural controls on Cu–Au mineralization in the Svappavaara area, northern Sweden: The northern continuation of the Nautanen IOCG-system (paper II), in: *Paleoproterozoic deformation in the Kiruna–Gällivare area in northern Norrbotten, Sweden: Setting, character, age, and control of iron oxide-apatite deposits*, PhD Thesis, edited by: Andersson, J. B. H., Luleå University of Technology, Luleå, Sweden, 15 pp., ISBN 978-91-7790-973-6, 978-91-7790-974-3, 2021.
- Bauer, T. E., Skyttä, P., Allen, R. L., and Weihed, P.: Syn-extensional faulting controlling structural inversion – Insights from the Palaeoproterozoic Vargfors syncline, Skellefte mining district, Sweden, *Precambrian Res.*, 191, 166–183, <https://doi.org/10.1016/j.precamres.2011.09.014>, 2011.
- Bauer, T. E., Andersson, J. B. H., Sarlus, Z., Lund, C., and Kearney, T.: Structural Controls on the Setting, Shape, and Hydrothermal Alteration of the Malmberget Iron Oxide-Apatite Deposit, Northern Sweden, *Econ. Geol.*, 113, 377–395, <https://doi.org/10.5382/econgeo.2018.4554>, 2018.
- Bauer, T. E., Lynch, E. P., Sarlus, Z., Dreijing-Carroll, D., Martinsson, O., Metzger, N., and Wanhainen, C.: Structural Controls on Iron Oxide Copper-Gold Mineralization and Related Alteration in a Paleoproterozoic Supracrustal Belt: Insights from the Nautanen Deformation Zone and Surroundings, Northern Sweden, *Econ. Geol.*, 117, 327–359, <https://doi.org/10.5382/econgeo.4862>, 2022.
- Bergman, S.: Geology of the northern Norrbotten ore province, northern Sweden, *Rapporter och Meddelanden 141*, Geol. Surv. of Swe., Uppsala, 428 pp., ISSN 0349-2176, ISBN 978-91-7403-393-9, 2018.
- Bergman, S. and Weihed, P.: Chapter 3 Archean (>2.6 Ga) and Paleoproterozoic (2.5–1.8 Ga), pre- and syn-orogenic magmatism, sedimentation and mineralization in the Norrbotten and Överkalix lithotectonic units, Sveco-Karelian orogen, Geological Society, London, *Memoirs*, 50, 27–81, <https://doi.org/10.1144/M50-2016-29>, 2020.
- Bergman, S., Kübler, L., and Martinsson, O.: Description of regional geological and geophysical maps of northern Norrbotten County (east of the Caledonian orogen), Ba 56, *Geol. Surv. of Swe.*, 110 pp., ISBN 91-7158-643-1, 2001.
- Bergman, S., Billström, K., Persson, P.-O., Skiöld, T., and Evins, P.: U-Pb age evidence for repeated Paleoproterozoic metamorphism and deformation near the Pajala shear zone in the northern Fennoscandian shield, *GFF*, 128, 7–20, <https://doi.org/10.1080/11035890601281007>, 2006.
- Bingen, B., Solli, A., Viola, G., Torgersen, E., Sandstad, J. S., Whitehouse, M. J., Røhr, T. S., Ganerød, M., and Nasuti, A.: Geochronology of the Palaeoproterozoic Kautokeino Greenstone

- Belt, Finnmark, Norway: Tectonic implications in a Fennoscandia context, *NJG*, 95, 365–396, <https://doi.org/10.17850/njg95-3-09>, 2015.
- Blomgren, H.: U-Pb Dating of Monazites from the Kiirunavaara and Rektorn Ore Deposits: Hydrothermal events affecting the Kiruna Main Ore, MSc thesis, University of Gothenburg, Gothenburg, 41 pp., ISSN 1400-3821, https://studentportal.gu.se/digitalAssets/1552/1552259_b891.pdf (last access: 1 December 2022), 2015.
- Cliff, R. A. and Rickard, D.: Isotope systematics of the Kiruna magnetite ores, Sweden; Part 2, Evidence for a secondary event 400 m.y. after ore formation, *Econ. Geol.*, 87, 1121–1129, <https://doi.org/10.2113/gsecongeo.87.4.1121>, 1992.
- Cliff, R. A., Rickard, D., and Blake, K.: Isotope systematics of the Kiruna magnetite ores, Sweden; Part 1, Age of the ore, *Econ. Geol.*, 85, 1770–1776, <https://doi.org/10.2113/gsecongeo.85.8.1770>, 1990.
- Corriveau, L., Montreuil, J.-F., and Potter, E. G.: Alteration Facies Linkages Among Iron Oxide Copper-Gold, Iron Oxide-Apatite, and Affiliated Deposits in the Great Bear Magmatic Zone, Northwest Territories, Canada, *Econ. Geol.*, 111, 2045–2072, <https://doi.org/10.2113/econgeo.111.8.2045>, 2016.
- Day, W. C., Slack, J. F., Ayuso, R. A., and Seeger, C. M.: Regional Geologic and Petrologic Framework for Iron Oxide ± Apatite ± Rare Earth Element and Iron Oxide Copper-Gold Deposits of the Mesoproterozoic St. Francois Mountains Terrane, Southeast Missouri, USA, *Econ. Geol.*, 111, 1825–1858, <https://doi.org/10.2113/econgeo.111.8.1825>, 2016.
- Frietsch, R.: Petrology of the Kurravaara area, northeast of Kiruna, northern Sweden, *Geological Survey of Sweden, C Series*, Uppsala, no. 760, 82 pp., 1979.
- Frietsch, R., Tuisku, P., Martinsson, O., and Perdahl, J.-A.: Early Proterozoic Cu-(Au) and Fe ore deposits associated with regional Na-Cl metasomatism in northern Fennoscandia, *Ore Geol. Rev.*, 12, 1–34, [https://doi.org/10.1016/S0169-1368\(96\)00013-3](https://doi.org/10.1016/S0169-1368(96)00013-3), 1997.
- Geijer, P.: Geology of the Kiruna District 2: Igneous rocks and iron ores of Kiirunavaara, Loussavaara and Toullavaara, Scientific and practical researches in Lapland arranged by Loussavaara-Kiirunavaara Aktiebolag, 278 pp., Kungliga boktryckeriet. P. A. Norstedt & Söner, Stockholm, 1910.
- Geijer, P.: Recent Developments at Kiruna, *Sveriges Geologiska Undersökning*, 22 pp., 1919.
- Geological Survey of Sweden: Berggrund 1 : 50 000–1 : 250 000 latest (shp) Bedrock, Geological Survey of Sweden [data set], <https://maps.slu.se/>, last access: 7 May 2019.
- Grigull, S., Berggren, R., Jönberger, J., Jönsson, C., Hellström, S., and Luth, S.: Folding observed in Paleoproterozoic supracrustal rocks in northern Sweden, in: *Geology of the northern Norrbotten ore province, northern Sweden*, edited by: Bergman, S., Rapport och Meddelanden 141, 205–258, *Geol. Surv. of Swe.*, Uppsala, ISSN 0349-2176, ISBN 978-91-7403-393-9, 2018.
- Groves, D. I., Bierlein, F. P., Meinert, L. D., and Hitzman, M. W.: Iron Oxide Copper-Gold (IOCG) Deposits through Earth History: Implications for Origin, Lithospheric Setting, and Distinction from Other Epigenetic Iron Oxide Deposits, *Econ. Geol.*, 105, 641–654, <https://doi.org/10.2113/gsecongeo.105.3.641>, 2010.
- Hietanen, A.: Generation of potassium-poor magmas in the northern Sierra Nevada and the Svecofennian of Finland, *J. Res. US Geol. Surv.*, 3, 631–645, 1975.
- Högdahl, K., Andersson, U. B., and Eklund, O.: The Transcandinavian Igneous Belt (TIB) in Sweden: a review of its character and evolution, *Special Paper 37, Geol. Surv. of Fin.*, Espoo, 125 pp., 2004.
- Lahtinen, R., Korja, R., and Nironen, M.: Paleoproterozoic tectonic evolution, in: *Precambrian Geology of Finland – key to the evolution of the Fennoscandian Shield*, Vol. 14, edited by: Lehtinen, M., Nurmi, P. A., and Rämö, O. T., Elsevier, Amsterdam, 481–532, ISBN 978-0-444-51421-9, 2005.
- Lantmateriet: Markhöjdmodell Nedladdning [data set], first version published in 2015, last updated 2022, <https://www.lantmateriet.se/sv/geodata/vara-produkter/produktlista/markhojdmodell-nedladdning/>, 2015.
- Lauri, L. S., Miles, J., Liu, X., and O'Brien, H.: Age and C-O isotopes of the hydrothermal breccias within the Kiruna-Naimakka zone, Norrbotten, Sweden, in: *Geological Society of Sweden 150 Year Anniversary Meeting*, edited by: Bergman Weihed, J., Johansson, Å., and Rehnström, E., *Geologiska Föreningens 150-års jubileum*, Uppsala, 17–19 August 2022, Abstract volume, *Geologiska Föreningen Specialpublikation 1*, 242–243, ISBN 978-91-987833-0-8, 2022.
- Lindblom, S., Broman, C., and Martinsson, O.: Magmatic-hydrothermal fluids in the Pahtohavare Cu-Au deposit in greenstone at Kiruna, Sweden, *Mineralium Deposita*, 31, 307–318, <https://doi.org/10.1007/BF02280794>, 1996.
- Logan, L., Andersson, J. B. H., Whitehouse, M. J., Martinsson, O., and Bauer, T. E.: Energy Drive for the Kiruna Mining District Mineral System(s): Insights from U-Pb Zircon Geochronology, *Minerals*, 12, 875–900, <https://doi.org/10.3390/min12070875>, 2022.
- Lundbohm, H. J.: Sketch of the Geology of the Kiruna district, *Geologiska Föreningen i Stockholm Förhandlingar*, 32, 751–788, <https://doi.org/10.1080/11035891009443831>, 1910.
- Luth, S., Jönsson, C., Grigull, S., Berggren, R., van Assema, B., Smoor, W., and Djuly, T.: The Pajala deformation belt in north east Sweden: Structural geological mapping and 3D modelling around Pajala, in: *Geology of the northern Norrbotten ore province, northern Sweden*, edited by: Bergman, S., Rapport och Meddelanden, 141, 287–310, *Geol. Surv. of Swe.*, Uppsala, 259–286, ISSN 0349-2176, ISBN 978-91-7403-393-9, 2018a.
- Luth, S., Jönberger, J., and Grigull, S.: The Vakko and Kovo Greenstone belts: Integrating structural geological mapping and geophysical modelling, in: *Geology of the northern Norrbotten ore province, northern Sweden*, edited by: Bergman, S., Rapport och Meddelanden, 141, 287–310, *Geol. Surv. of Swe.*, Uppsala, ISSN 0349-2176, ISBN 978-91-7403-393-9, 2018b.
- Lynch, E. P., Jönberger, J., Bauer, T. E., Sarlus, Z., and Martinsson, O.: Meta-volcanosedimentary rocks in the Nautanen area, Norrbotten: preliminary lithological and deformation characteristics, *SGU-rapport 30, Geol. Surv. of Swe.*, Uppsala, 51 pp., 2015.
- Martinsson, O.: Tectonic Setting and Metallogeny of the Kiruna Greenstones, PhD thesis, Luleå tekniska universitet, Luleå, Sweden, 162 pp., ISSN: 1402–1544, <http://ltu.diva-portal.org/smash/record.jsf?pid=diva2:999505&dsid=-2131> (last access: 19 May 2023), 1997.

- Martinsson, O.: Geology and Metallogeny of the Northern Norrbotten Fe-Cu-Au Province, in: Svecofennian ore-forming environments of northern Sweden- volcanic associated Zn-Cu-Au-Ag, intrusion related Cu-Au, sediment hosted Pb-Zn, and magnetite-apatite deposits in northern Sweden, edited by: Allen, R. L., Martinsson, O., and Weihed, P., Society of Economic Geologists, 131–148, ISBN 1-887483-33-0, 2004.
- Martinsson, O.: Genesis of the Per Geijer apatite iron ores, Kiruna area, northern Sweden, SGA biennial meeting 2015, Nancy, France, 24–27 August <https://e-sga.org/nc/publications/sga-biennial-meetings-abstract-volumes/2015-nancy/> (last access: 10 March 2022), 2015.
- Martinsson, O. and Hansson, K.-E.: Apatite Iron Ores in the Kiruna Area, in: Svecofennian ore-forming environments of northern Sweden- volcanic associated Zn-Cu-Au-Ag, intrusion related Cu-Au, sediment hosted Pb-Zn, and magnetite-apatite deposits in northern Sweden, Society of Economic Geologists, 33, 173–175, 2004.
- Martinsson, O. and Perdahl, J.-A.: Paleoproterozoic extensional and compressional magmatism in northern Norrbotten, northern Sweden (Paper II), in: Svecofennian volcanism in northernmost Sweden, PhD Thesis, edited by: Perdahl, J.-A., Luleå University of Technology, Luleå, Sweden, 161 pp., <https://ltu.diva-portal.org/smash/record.jsf?pid=diva2:991040&dsid=4905> (last access: 29 March 2022), 1995.
- Martinsson, O., Perdahl, J.-A., and Bergman, J.: Greenstone and porphyry hosted ore deposits in northern Norrbotten, Research Programme Ore Geology Related to Prospecting Report 92-00752P, Närings- och teknikutvecklingsverket, Uppsala, 78 pp., 1993.
- Martinsson, O., Hallberg, A., Söderholm, K., and Billström, K.: Pahtohavare – an epigenetic Cu-Au deposit in the Paleoproterozoic Kiruna Greenstones (Paper III), in: Tectonic Setting and Metallogeny of the Kiruna Greenstones, PhD thesis, edited by: Martinsson, O., Luleå University of Technology, Luleå, Sweden, 37 pp., ISSN 1402-1544, <http://ltu.diva-portal.org/smash/record.jsf?pid=diva2:999505&dsid=-2131> (last access: 19 May 2023), 1997a.
- Martinsson, O., Hallberg, A., Broman, C., Godin-Jonasson, L., Kisiel, T., and Fallick, A. E.: Viscaria – a syngenetic exhalative Cu-deposit in the Paleoproterozoic Kiruna Greenstones (Paper II), in: Tectonic Setting and Metallogeny of the Kiruna Greenstones, PhD Thesis, edited by: Martinsson, O., Luleå University of Technology, Luleå, Sweden, 57 pp., ISSN 1402-1544, <http://ltu.diva-portal.org/smash/record.jsf?pid=diva2:999505&dsid=-2131> (last access: 19 May 2023), 1997b.
- Martinsson, O., Vaasjoki, M., and Persson, P.-O.: U-Pb zircon ages of Archaean to Palaeoproterozoic granitoids in the Torneträsk–Råstojaure area, northern Sweden, in: Radiometric dating results 4, Geological Survey of Sweden, series C, no. 831, Uppsala, 70–90, ISSN 1103-3371, ISBN 91-7158-604-0, <http://resource.sgu.se/produkter/c/831-rapport.pdf> (last access: 21 November 2021), 1999.
- Martinsson, O., Billström, K., Broman, C., Weihed, P., and Wanhainen, C.: Metallogeny of the Northern Norrbotten Ore Province, northern Fennoscandian Shield with emphasis on IOCG and apatite-iron ore deposits, *Ore Geol. Rev.*, 78, 447–492, <https://doi.org/10.1016/j.oregeorev.2016.02.011>, 2016.
- Martinsson, O., Bergman, S., Persson, P.-O., Schöberg, H., Billström, K., and Shumlyanskyy, L.: Stratigraphy and ages of Palaeoproterozoic metavolcanic and metasedimentary rocks at Käymäjärvi, northern Sweden, in: Geology of the northern Norrbotten ore province, northern Sweden, edited by: Bergman, S., Rapport och Meddelanden, 141, Geol. Surv. of Swe., Uppsala, 79–106, 287–310, ISSN 0349-2176, ISBN 978-91-7403-393-9, 2018.
- Mellqvist, C.: The Archaean–Proterozoic Palaeoboundary in the Luleå area, northern Sweden: field and isotope geochemical evidence for a sharp terrane boundary, *Precambrian Res.*, 96, 225–243, [https://doi.org/10.1016/S0301-9268\(99\)00011-X](https://doi.org/10.1016/S0301-9268(99)00011-X), 1999.
- Naslund, H. R., Henríquez, F., Nyström, J. O., Vivallo, W., and Dobbs, F. M.: Magmatic iron ores and associated mineralisation: Examples from the Chilean High Andes and Coastal Cordillera, in: Hydrothermal Iron Oxide-Copper-Gold & Related Deposits: A Global Perspective, vol. 2, edited by: Porter, T. M., PCG Publishing, Adelaide, 207–226, ISBN 0987119621, 9780987119629, 2002.
- Nyström, J. O. and Henriquez, F.: Magmatic features of iron ores of the Kiruna type in Chile and Sweden; ore textures and magnetite geochemistry, *Econ. Geol.*, 89, 820–839, <https://doi.org/10.2113/gsecongeo.89.4.820>, 1994.
- Offerberg, J.: Berggrundsgeologiska och flygmagnetiska kartbladen, Kiruna NV, NO, SV, SO, Sveriges Geologiska Undersökning, Stockholm, ISSN 0586-1543, 1967.
- Öhlander, B., Skiöld, T., Elming, S.-Å., Claesson, S., and Nisca, D. H.: Delineation and character of the Archaean-Proterozoic boundary in northern Sweden, *Precambrian Res.*, 64, 67–84, [https://doi.org/10.1016/0301-9268\(93\)90069-E](https://doi.org/10.1016/0301-9268(93)90069-E), 1993.
- Parák, T.: The origin of the Kiruna iron ores, Sveriges Geologiska Undersökning Ser. C, Nr. 709, Årsbok 69, Nr. 1, C. Davidsons Boktryckeri AB, Stockholm, 209 pp., ISBN 978-91-7158-069-6, 1975.
- Perdahl, J.-A. and Frietsch, R.: Petrochemical and petrological characteristics of 1.9 Ga old volcanics in northern Sweden, *Precambrian Res.*, 64, 239–252, [https://doi.org/10.1016/0301-9268\(93\)90079-H](https://doi.org/10.1016/0301-9268(93)90079-H), 1993.
- Pharaoh, T. C. and Pearce, J. A.: Geochemical evidence for the geotectonic setting of early Proterozoic metavolcanic sequences in Lapland, *Precambrian Res.*, 25, 283–308, [https://doi.org/10.1016/0301-9268\(84\)90037-8](https://doi.org/10.1016/0301-9268(84)90037-8), 1984.
- Reich, M., Simon, A. C., Deditius, A., Barra, F., Chryssoulis, S., Lagas, G., Tardani, D., Knipping, J., Bilenker, L., Sanchez-Alfaro, P., Roberts, M. P., and Munizaga, R.: Trace element signature of pyrite from the Los Colorados iron oxide-apatite (IOA) deposit, Chile; a missing link between Andean IOA and iron oxide copper-gold systems?, *Econ. Geol. and the Bulletin of the Society of Economic Geologists*, 111, 743–761, <https://doi.org/10.2113/econgeo.111.3.743>, 2016.
- Reich, M., Simon, A. C., Barra, F., Palma, G., Hou, T., and Bilenker, L. D.: Formation of iron oxide-apatite deposits, *Nat. Rev. Earth Environ.*, 3, 758–775, <https://doi.org/10.1038/s43017-022-00335-3>, 2022.
- Romer, R. L.: U-Pb systematics of stilbite-bearing low-temperature mineral assemblages from the Malmberget iron ore, northern Sweden, *Geochim. Cosmochim. Ac.*, 60, 1951–1961, 1996.
- Romer, R. L., Martinsson, O., and Perdahl, J. A.: Geochronology of the Kiruna iron ores and hydrothermal alterations, *Econ. Geol.*,

- 89, 1249–1261, <https://doi.org/10.2113/gsecongeo.89.6.1249>, 1994.
- Sarlus, Z., Andersson, U. B., Bauer, T. E., Wanhainen, C., Martinsson, O., Nordin, R., and Andersson, J. B. H.: Timing of plutonism in the Gällivare area: implications for Proterozoic crustal development in the northern Norrbotten ore district, Sweden, *Geol. Mag.*, 155, 1351–1376, <https://doi.org/10.1017/S0016756817000280>, 2018.
- Sarlus, Z., Andersson, U. B., Martinsson, O., Bauer, T. E., Wanhainen, C., Andersson, J. B. H., and Whitehouse, M. J.: Timing and origin of the host rocks to the Malmberget iron oxide-apatite deposit, Sweden, *Precambrian Res.*, 342, 105652, <https://doi.org/10.1016/j.precamres.2020.105652>, 2020.
- SGUs Kartvisare: Sveriges Geologiska Undersökning, Uppsala. <https://apps.sgu.se/kartvisare/>, last access: 1 June 2022.
- Sillitoe, R. H.: Iron oxide-copper-gold deposits: an Andean view, *Mineralium Deposita*, 38, 787–812, <https://doi.org/10.1007/s00126-003-0379-7>, 2003.
- Simon, A. C., Knipping, J., Reich, M., Barra, F., Deditius, A. P., Bilinker, L., and Childress, T.: Kiruna-Type Iron Oxide-Apatite (IOA) and Iron Oxide Copper-Gold (IOCG) Deposits Form by a Combination of Igneous and Magmatic-Hydrothermal Processes: Evidence from the Chilean Iron Belt, in: *Metals, Minerals, and Society*, Society of Economic Geologists (SEG), <https://doi.org/10.5382/SP.21.06>, 2018.
- Skelton, A., Mansfeld, J., Ahlin, S., Lundqvist, T., Linde, J., and Nilsson, J.: A compilation of metamorphic pressure–temperature estimates from the Svecofennian province of eastern and central Sweden, *GFF*, 140, 1–10, <https://doi.org/10.1080/11035897.2017.1414074>, 2018.
- Skiöld, T.: Implications of new U–Pb zircon chronology to early Proterozoic crustal accretion in northern Sweden, *Precambrian Res.*, 38, 147–164, [https://doi.org/10.1016/0301-9268\(88\)90089-7](https://doi.org/10.1016/0301-9268(88)90089-7), 1988.
- Skirrow, R. G.: Iron oxide copper-gold (IOCG) deposits – a review (part 1): settings, mineralogy, ore geochemistry, and classification, *Ore Geol. Rev.*, 104569, <https://doi.org/10.1016/j.oregeorev.2021.104569>, 2021.
- Skyttä, P., Bauer, T. E., Tavakoli, S., Hermansson, T., Andersson, J., and Weihed, P.: Pre-1.87Ga development of crustal domains overprinted by 1.87Ga transpression in the Palaeoproterozoic Skellefte district, Sweden, *Precambrian Res.*, 206–207, 109–136, <https://doi.org/10.1016/j.precamres.2012.02.022>, 2012.
- Skyttä, P., Piippo, S., Kloppenburg, A., and Corti, G.: 2.45 Ga break-up of the Archaean continent in Northern Fennoscandia: Rifting dynamics and the role of inherited structures within the Archaean basement, *Precambrian Res.*, 324, 303–323, <https://doi.org/10.1016/j.precamres.2019.02.004>, 2019.
- Skyttä, P., Määttä, M., Palsatech Oy, Piippo, S., Kara, J., Käpyaho, A., Heilimo, E., and O’Brien, H.: Constraints over the age of magmatism and subsequent deformation for the Neoproterozoic Kukkola Gneiss Complex, northern Fennoscandia, *Bull. Geol. Soc. Finl.*, 92, 19–38, <https://doi.org/10.17741/bgsf/92.1.002>, 2020.
- Smith, M., Coppard, J., Herrington, R., and Stein, H.: The Geology of the Rakkurijärvi Cu–(Au) Prospect, Norrbotten: A New Iron Oxide-Copper-Gold Deposit in Northern Sweden, *Econ. Geol.*, 102, 393–414, <https://doi.org/10.2113/gsecongeo.102.3.393>, 2007.
- Smith, M., Coppard, J., and Herrington, R.: The geology of the Rakkurijärvi copper-prospect, Norrbotten county, Sweden, in: *Hydrothermal Iron Oxide Copper-Gold and Related Deposits: A Global Perspective*, vol. 4, edited by: Porter, T. M., PGC Publishing, Adelaide, 427–440, ISBN 0987119621, 9780987119629, 2010.
- Smith, M. P., Storey, C. D., Jeffries, T. E., and Ryan, C.: In Situ U–Pb and Trace Element Analysis of Accessory Minerals in the Kiruna District, Norrbotten, Sweden: New Constraints on the Timing and Origin of Mineralization, *J. Petrol.*, 50, 2063–2094, <https://doi.org/10.1093/petrology/egp069>, 2009.
- Storey, C. D., Smith, M. P., and Jeffries, T. E.: In situ LA-ICP-MS U–Pb dating of metavolcanics of Norrbotten, Sweden: Records of extended geological histories in complex titanite grains, *Chem. Geol.*, 240, 163–181, <https://doi.org/10.1016/j.chemgeo.2007.02.004>, 2007.
- Tornos, F.: Magnetite-Apatite and IOCG deposits formed by magmatic-hydrothermal evolution of complex calc-alkaline melts, in: *Eleventh Biennial SGA Meeting, Let’s talk ore deposits*, Antofagasta, Chile, 26–29 September 2011, <https://e-sga.org/nc/publications/sga-biennial-meetings-abstract-volumes/2011-antofagasta/> (last access: 1 December 2022), 2011.
- Tornos, F., Velasco, F., and Hanchar, J. M.: The Magmatic to Magmatic-Hydrothermal Evolution of the El Laco Deposit (Chile) and Its Implications for the Genesis of Magnetite-Apatite Deposits, *Econ. Geol.*, 112, 1595–1628, <https://doi.org/10.5382/econgeo.2017.4523>, 2017.
- Troll, V. R., Weis, F. A., Jonsson, E., Andersson, U. B., Majidi, S. A., Högdahl, K., Harris, C., Millet, M.-A., Chinnasamy, S. S., Kooijman, E., and Nilsson, K. P.: Global Fe–O isotope correlation reveals magmatic origin of Kiruna-type apatite-iron-oxide ores, *Nat. Commun.*, 10, 1712, <https://doi.org/10.1038/s41467-019-09244-4>, 2019.
- Velasco, F., Tornos, F., and Hanchar, J. M.: Immiscible iron- and silica-rich melts and magnetite geochemistry at the El Laco volcano (northern Chile): Evidence for a magmatic origin for the magnetite deposits, *Ore Geol. Rev.*, 79, 346–366, <https://doi.org/10.1016/j.oregeorev.2016.06.007>, 2016.
- Vollmer, F. W., Wright, S. F., and Hudleston, P. J.: Early deformation in the Svecofennian greenstone belt of the Kiruna iron district, northern Sweden, *Geologiska Föreningen i Stockholm Förhandlingar*, 106, 109–118, <https://doi.org/10.1080/11035898409454620>, 1984.
- Wanhainen, C., Billström, K., Martinsson, O., Stein, H., and Nordin, R.: 160 Ma of magmatic/hydrothermal and metamorphic activity in the Gällivare area: Re–Os dating of molybdenite and U–Pb dating of titanite from the Aitik Cu–Au–Ag deposit, northern Sweden, *Miner Deposita*, 40, 435–447, <https://doi.org/10.1007/s00126-005-0006-x>, 2005.
- Wanhainen, C., Broman, C., Martinsson, O., and Magnor, B.: Modification of a Palaeoproterozoic porphyry-like system: Integration of structural, geochemical, petrographic, and fluid inclusion data from the Aitik Cu–Au–Ag deposit, northern Sweden, *Ore Geol. Rev.*, 48, 306–331, <https://doi.org/10.1016/j.oregeorev.2012.05.002>, 2012.
- Weihed, P. and Williams, P. J.: Metallogeny of the northern Fennoscandian Shield: a set of papers on Cu–Au and VMS

- deposits of northern Sweden, *Miner Deposita*, 40, 347–350, <https://doi.org/10.1007/s00126-005-0022-x>, 2005.
- Weihed, P., Billström, K., Persson, P.-O., and Weihed, J. B.: Relationship between 1.90–1.85 Ga accretionary processes and 1.82–1.80 Ga oblique subduction at the Karelian craton margin, Fennoscandian Shield, *GFF*, 124, 163–180, <https://doi.org/10.1080/11035890201243163>, 2002.
- Welin, E.: The depositional evolution of the Svecofennian supracrustal sequence in Finland and Sweden, *Precambrian Res.*, 35, 95–113, [https://doi.org/10.1016/0301-9268\(87\)90047-7](https://doi.org/10.1016/0301-9268(87)90047-7), 1987.
- Westhues, A., Hanchar, J. M., Whitehouse, M. J., and Martinsson, O.: New Constraints on the Timing of Host-Rock Emplacement, Hydrothermal Alteration, and Iron Oxide-Apatite Mineralization in the Kiruna District, Norrbotten, Sweden, *Econ. Geol.*, 111, 1595–1618, <https://doi.org/10.2113/econgeo.111.7.1595>, 2016.
- Westhues, A., Hanchar, J. M., Voisey, C. R., Whitehouse, M. J., Rossman, G. R., and Wirth, R.: Tracing the fluid evolution of the Kiruna iron oxide apatite deposits using zircon, monazite, and whole rock trace elements and isotopic studies, *Chem. Geol.*, 466, 303–322, <https://doi.org/10.1016/j.chemgeo.2017.06.020>, 2017.
- Williams, P. J., Barton, M. D., Johnson, D. A., Fontboté, L., Haller, A. de, Mark, G., Oliver, N. H. S., and Marschik, R.: Iron Oxide Copper-Gold Deposits - Geology, Space-Time Distribution, and Possible Modes of Origin, in: *One Hundredth Anniversary Volume*, Society of Economic Geologists, Littleton, USA, 371–405, <https://doi.org/10.5382/AV100.13>, 2005.
- Witschard, F.: The geological and tectonic evolution of the Precambrian of northern Sweden – A case for basement reactivation?, *Precambrian Res.*, 23, 273–315, [https://doi.org/10.1016/0301-9268\(84\)90047-0](https://doi.org/10.1016/0301-9268(84)90047-0), 1984.
- Wright, S.: Early Proterozoic Deformational History of the Kiruna District, Northern Sweden, PhD thesis, University of Minnesota, 170 pp., <https://www.proquest.com/openview/13779d86ccd27559cce776fe5bc52fe8/1?pq-origsite=gscholar&cbl=18750&diss=y> (last access: 19 May 2023), 1988.
- Wyborn, L. A. I., Heinrich, C. A., and Jaques, A. L.: Australian Proterozoic Mineral Systems: Essential Ingredients and Mappable Criteria, in: *Australasian Institute of Mining and Metallurgy Publication Series, the AusIMM Annual Conference, Darwin, Australia, 5–9 August 1994*, 109–115, <https://www.ausimm.com/publications/conference-proceedings/1994-ausimm-annual-conference-darwin-august-1994/> (last access: 19 May 2023), 1994.